SANDIA REPORT
SAND200X-XXXX
Unlimited Release
Printed August 2016

TDAAPS 2: Acoustic Wave Propagation in Attenuative Moving Media

Leiph A. Preston

Prepared by
Sandia National Laboratories
Albuquerque, New Mexico 87185 and Livermore, California 94550

Sandia National Laboratories is a multi-program laboratory managed and operated by Sandia Corporation, a wholly owned subsidiary of Lockheed Martin Corporation, for the U.S. Department of Energy's National Nuclear Security Administration under contract DE-AC04-94AL85000.

Issued by Sandia National Laboratories, operated for the United States Department of Energy by Sandia Corporation.

Available to DOE and DOE contractors from
U.S. Department of Energy
Office of Scientific and Technical Information
P.O. Box 62
Oak Ridge, TN 37831

Telephone: (865) 576-8401
Facsimile: (865) 576-5728
E-Mail: reports@osti.gov
Online ordering: http://www.osti.gov/scitech

Available to the public from
U.S. Department of Commerce
National Technical Information Service
5301 Shawnee Rd
Alexandria, VA 22312

Telephone: (800) 553-6847
Facsimile: (703) 605-6900
E-Mail: orders@ntis.gov
Online order: http://www.ntis.gov/search

SAND200X-XXXX
Unlimited Release
Printed August 2016

TDAAPS 2: Acoustic Wave Propagation in Attenuative Moving Media

Leiph A. Preston
Department of Geophysics
Sandia National Laboratories
P.O. Box 5800 MS 0750
Albuquerque, New Mexico 87185-0750

Abstract

This report outlines recent enhancements to the TDAAPS algorithm first described by Symons et al., 2005. One of the primary additions to the code is the ability to specify an attenuative media using standard linear fluid mechanisms to match reasonably general frequency versus loss curves, including common frequency versus loss curves for the atmosphere and seawater. Other improvements that will be described are the addition of improved numerical boundary conditions via various forms of Perfectly Matched Layers, enhanced accuracy near high contrast media interfaces, and improved physics options.

ACKNOWLEDGMENTS

The author would like to acknowledge the many individuals from many organizations that make the Source Physics Experiment possible. The author also wishes to thank the National Nuclear Security Administration's office of Defense Nuclear Nonproliferation Research and Development (DNN R&D) for their sponsorship of the Source Physics Experiment working group and this research.

CONTENTS

TDAAPS 2: Acoustic Wave Propagation in Attenuative Moving Media..... 3
1. Introduction.....9
2. Attenuation.....13
3. Absorbing Boundary Conditions..... 25
4. Physics Improvements..... 35
5. Determining Attenuation Parameters.....39
6. Validation Tests..... 43
7. Conclusions.....51
8. References.....53
Distribution..... 55

FIGURES

Figure 1: Spatial discretization of the numerical volume for TDAAPS.....10
Figure 2: Generic grid cell..... 11
Figure 3: Comparison of Sponge and CPML absorbing boundary conditions for the X-component of particle velocity.....32
Figure 4: Comparison of Sponge and CPML for Z-component of particle velocity..... 32
Figure 5: Comparison of Sponge and CPML for pressure..... 33
Figure 6: Demonstration of CPML performance in a homogeneous model on the XZ plane for pressure..... 34
Figure 7: Effects of using all the first order terms in a realistic atmospheric model. "Standard" refers to the usual method of neglecting terms, whereas "added terms" refers to the inclusion of all first order terms. The right inset shows a 10x enlargement of the tail end of the primary pulse and coda..... 38
Figure 8: Acoustic attenuation factor fits for a 1 and 2 mechanism model..... 40
Figure 9: Sound speed dispersion implied by the 2 mechanism model.....41
Figure 10: Seawater attenuation factor fits for 1 and 2 mechanism attenuation models.....42
Figure 11: X-component of velocity comparison for fixed acoustic models.....43
Figure 12: Z-component of velocity comparison for fixed acoustic model.....44
Figure 13: Pressure comparison for fixed acoustic model.....44
Figure 14: X-component velocity comparison with wind model..... 45
Figure 15: Y-component of velocity comparison for wind model..... 46

Figure 16: Z-component of velocity comparison for wind model.....46
Figure 17: Pressure comparison for wind model.....47
Figure 18: X-component of velocity comparison for attenuative model.....48
Figure 19: Z-component of velocity comparison for attenuative model.....49
Figure 20: Pressure comparison for attenuative model.....49

NOMENCLATURE

DOE	Department of Energy
SNL	Sandia National Laboratories
TDAAPS	Time-Domain Atmospheric Acoustic Propagation Suite
PML	Perfectly Matched Layer
CPML	Convolutional Perfectly Matched Layer
MPML	Multiaxial Perfectly Matched Layer

1. INTRODUCTION

The Time-Domain Atmospheric Acoustic Suite, TDAAPS, was originally described in Symons et al., 2005. This suite of algorithms simulates 3-D linear acoustic wave propagation within a moving media acoustic model. It was originally designed with atmospheric acoustics with wind as the primary media of interest. However, it is not restricted to that domain. Any acoustic application with a moving (or stationary) media where linear wave propagation is a good approximation is applicable, including hydroacoustics.

This report will briefly summarize the main characteristics of the TDAAPS algorithm in the introduction. In subsequent sections, it will describe major new features of the algorithm, including the addition of attenuation, PML numerical boundaries, increased stability and accuracy near high contrast material interfaces such as at the air-earth boundary, and enhanced physics in the pressure updating equations.

This introduction is meant only to give the necessary background for TDAAPS that will be built upon in later sections. For more detailed information on TDAAPS, please see the original TDAAPS SAND report (Symons et al., 2005).

1.1. Non-Attenunative Moving Acoustic Equations

The original TDAAPS algorithm solves the non-attenuative, linearized, coupled set of first-order differential equations for an inviscid fluid with the dependent variables perturbation pressure, $p(\vec{x},t)$, and the three components of the perturbed material particle velocity vector, $\vec{w}(\vec{x},t)$. The ambient medium wind vector $\vec{v}(\vec{x})$, the bulk modulus $\kappa(\vec{x})$, and density $\rho(\vec{x})$ are functions of 3-D position but not of time. Of course, the atmosphere, for example, is actually changing as a function of time as well and TDAAPS does have the ability to use time-varying media. However, throughout this report, I will assume that the change in medium over the duration of wave propagation is small and can be ignored, for simplicity.

The coupled velocity-pressure first-order system of equations with moving media are:

$$\begin{aligned} \frac{\partial w_i}{\partial t}+\frac{1}{\rho}\frac{\partial p}{\partial x_i}+w_j\frac{\partial v_i}{\partial x_j}+v_j\frac{\partial w_i}{\partial x_j}&=\frac{1}{\rho}f_i \\ \frac{\partial p}{\partial t}+\kappa\frac{\partial w_j}{\partial x_j}+v_j\frac{\partial p}{\partial x_j}&=\frac{\partial e}{\partial t} \end{aligned} \tag{1}$$

Using Einstein summation convention for repeated indices; $\vec{f}$ are the force sources and e are the energy density sources corresponding to moment density sources. Note that the first two terms on the lefthand sides of the equations are the terms associated with a fixed (stationary media) acoustic wave propagation. The first two terms on the lefthand side of the pressure equation (second equation of Equation 1) is derived from the pressure-volumetric strain constitutive relationship.

1.2 Finite-Difference Formulation

TDAAPS utilizes a standard staggered grid in space and a double-time-step approach to solving equation (1) on a discrete, regular, rectangular grid. In this volume discretization the left, back, top corner corresponds to x_{min}, y_{min}, z_{min} with grid points equally spaced in each dimension with spacing d_x, d_y, d_z, respectively, and number of grid nodes of I, J, K (Figure 1). In the standard staggered grid, the pressure nodes are located at the corners of a cell and the velocity components are located on edge mid-points in order to allow centered finite differencing (Figure 2). All medium parameters (wind, bulk modulus, and density) are co-located with the pressure nodes. Due to the fact that pressure and velocity component equations also contain those self-same dependent variables, the equations would normally be solved via implicit time marching methods. However, TDAAPS uses a double-time-step approach. In this approach there are actually two sets of dependent variables. One set lives on even time step points and the other lives on odd time step points. This allows explicit time stepping with centered time derivatives. The cost is extra memory usage and, once numerical boundary conditions are imposed, a more strict time step requirement. Time updating also uses a staggered time step approach, with pressure updating on integer time steps and velocities updating on half-integer time steps.

Equation 1 is solved using 2nd order accurate temporal and 4th order accurate spatial finite-difference operators. By default standard Taylor series coefficients are used for the respective operators, but the user may input operators of his or her choice in order to optimize performance in certain situations.

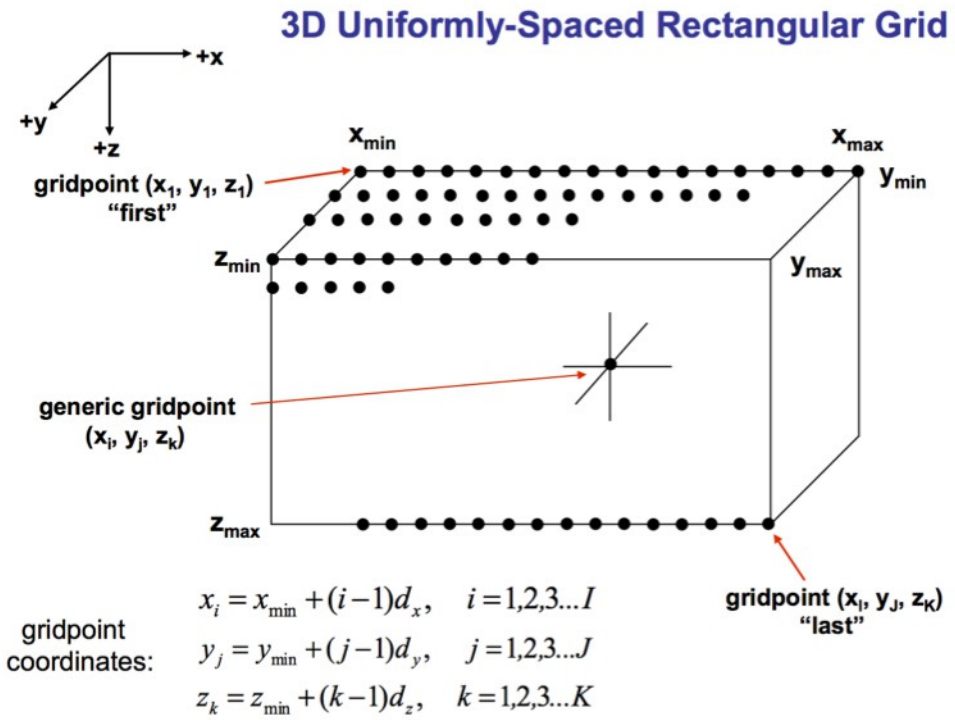

Figure 1: Spatial discretization of the numerical volume for TDAAPS

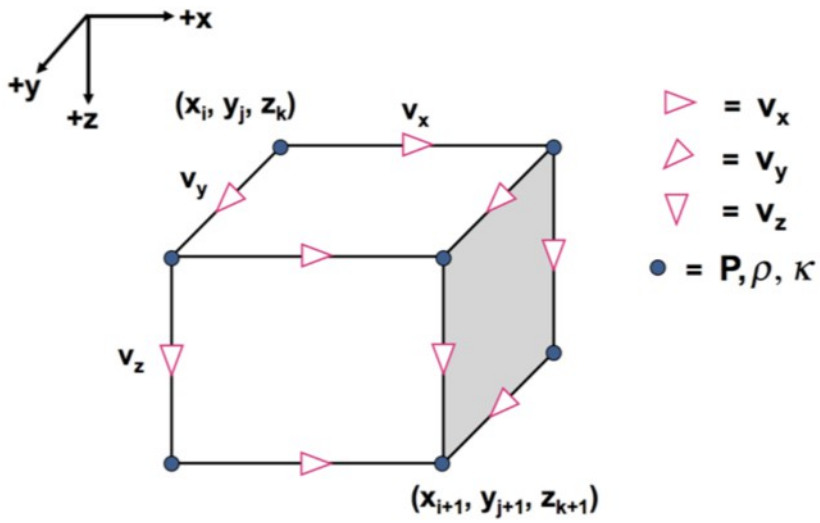

Figure 2: Generic grid cell

2. ATTENUATION

2.1 Introduction

Attenuation refers to the loss of energy from the propagating wavefield into some other form of energy, such as heat, molecular dissipation, or any irreversible process. Geometric spreading, reflection, refraction, and wavefield scattering are already included in the general non-attenuative equations given in Equation 1 and are not considered "attenuation" in this report. However, it should be remarked that scattering of the wavefield on a smaller scale than is resolvable numerically could be attempted to be modeled as an attenuation process in certain circumstances.

2.2 Mathematical Formulation

We borrow the idea of a standard linear solid from the seismological literature (e.g., Aki and Richards, 2002) and implement a so-called standard linear fluid in order to simulate attenuation in TDAAPS. We still retain the assumption of an inviscid fluid, but allow attenuation of the compressional components. This report closely follows the notation and derivation of the equations as described in Aldridge (in prep) for the full elastic standard linear solid system.

The physical idea of a standard linear solid/fluid is that of a spring and dashpot in series. When one pulls on the system, there is an immediate response due to the spring, followed by a slower relaxation due to the dashpot. Mathematically this can be represented as a delta function followed by a one-sided decaying exponential, defining a single standard linear fluid mechanism or rate-of-relaxation function. Adding together several standard linear fluid mechanisms, one obtains the full attenuation model. To incorporate this idea, we generalize the pressure (P) - volumetric strain (ε) relationship (the first two terms on the lefthand side of the second equation in Equation 1) to be a convolution of the strain tensor with time-dependent medium parameters (K)

$$P(\vec{x},t) = -\mathrm{K}(\vec{x},t) * \varepsilon(\vec{x},t) \tag{2}$$

Where we define K according to the assumed functional form

$$\mathrm{K}(\vec{x},t) = \kappa(\vec{x})\left[\delta(t) - \sum_{r=1}^{R} a_r(\vec{x})\,\omega_r(\vec{x})\exp(-\omega_r(\vec{x})t)\,H(t)\right] \tag{3}$$

Where κ is the bulk modulus at infinite frequency, $\delta(t)$ is the delta function, and $H(t)$ is the Heavyside step function. There are R rate-of-relaxation functions in this attenuation model. Each rate-of-relaxation function is defined by two parameters, $a_r(\vec{x})$ and $\omega_r(\vec{x})$, which are the amplitude scalar and relaxation frequency, respectively, for the mechanism. Note that these two parameters can be functions of 3-D space.

A favorable aspect of the above equations is that they can be relatively efficiently implemented in a time-domain algorithm such as TDAAPS. To do this, first we plug Equation 3 into Equation 2 and then time-differentiate the resulting equation, giving

$$\frac{\partial P(\vec{x},t)}{\partial t} = -\kappa(\vec{x})\frac{\partial w_k(\vec{x},t)}{\partial x_k} - \kappa(\vec{x})\sum_{r=1}^{R} p_r(\vec{x},t) \tag{4}$$

where $p_r(\vec{x},t)$ is a memory variable defined by

$$p_r(\vec{x},t) = -a_r(\vec{x})\omega_r(\vec{x})\exp(-\omega_r(\vec{x})t)H(t)\frac{\partial w_k(\vec{x},t)}{\partial x_k} \tag{5}$$

Differentiating the memory variable equation with respect to time, one obtains

$$\frac{\partial p_r(\vec{x},t)}{\partial t} + \omega_r(\vec{x})p_r(\vec{x},t) + a_r(\vec{x})\omega_r(\vec{x})\frac{\partial w_k(\vec{x},t)}{\partial x_k} = 0 \tag{6}$$

Comparing Equation 4 and the second line (pressure equation) of Equation 1, one notices that the second term of equation 4 is the only term that needs added. In addition to that term, a set of R partial differential equations, given by Equation 6, is augmented to the original system to give a new set of linear, first-order partial differential equations called the velocity-memory-pressure system of equations. To reiterate, the new set of equations are the R equations defined by Equation 6, plus the modified form of Equation 1:

$$\begin{aligned} &\frac{\partial w_i(\vec{x},t)}{\partial t} + \frac{1}{\rho(\vec{x})}\frac{\partial P(\vec{x},t)}{\partial x_i} + w_j(\vec{x},t)\frac{\partial v_i(\vec{x})}{\partial x_j} + v_j(\vec{x})\frac{\partial w_i(\vec{x},t)}{\partial x_j} = \frac{1}{\rho(\vec{x})}f_i(\vec{x},t) \\ &\frac{\partial P(\vec{x},t)}{\partial t} + \kappa(\vec{x})\frac{\partial w_j(\vec{x},t)}{\partial x_j} + \kappa(\vec{x})\sum_{r=1}^{R} p_r(\vec{x},t) + v_j(\vec{x})\frac{\partial P(\vec{x},t)}{x_j} = \frac{\partial e(\vec{x},t)}{\partial t} \end{aligned} \tag{7}$$

2.3 Numerical Implementation

Equations 6 and 7 represent the system of equations TDAAPS solves for an attenuative moving acoustic inviscid fluid for linearized acoustic wave propagation. The discretization in space and time is precisely the same as for the non-attenuative case described in Section 1. The one addition is that there will be 2*R 3-D memory variables: one set of R for even time steps and a second set of R for the odd time steps, just as the other dependent variables. The memory variables are stored in the same locations as the pressure variables and are updated concurrently with pressure. The attenuation model consists of N_m piece-wise homogeneous non-overlapping regions that cover the entire 3-D model domain. Each 3-D pressure grid point in the model has an index $(0 \ldots N_m - 1)$ that associates it with one of the N_m sets of R ω_r and a_r parameters.

In the following sections, we will document the finite-difference forms of the system of equations given in Equations 6 and 7. First, however, we will non-dimensionalize the system of equations.

2.3.1 Non-Dimensional Formulation

This derivation closely follows the formulations outlined in Aldridge and Haney (2008) for the elastic system of equations and in Aldridge (in prep) for the acoustic equations. Define characteristic units for sound speed and density as S_c and S_ρ, respectively. Then non-dimensional sound speed and density are defined as

$$\hat{c}(\vec{x},t)=\frac{c(\vec{x},t)}{S_c}$$

$$\hat{\rho}(\vec{x},t)=\frac{\rho(\vec{x},t)}{S_\rho}$$

Also, defining S_w and S_P as the units for particle velocities and pressure, one can complete the system of non-dimensional equations with an equation relating the four characteristic units. In a stationary acoustic whole space in the far field the pressure from a point source will be related to the radial particle velocity, w_r via

$$P=\rho c\, w_r$$

suggesting that the appropriate relationship among the four characteristic units should be $S_P=S_\rho S_c S_w$. With these definitions, the remaining independent and dependent variables in non-dimensional form are:

$$\hat{\kappa}(\vec{x},t)=\frac{\kappa(\vec{x},t)}{S_\rho S_c^2},\ \hat{v}_x(\vec{x},t)=\frac{v_x(\vec{x},t)}{S_c},\ \hat{v}_y(\vec{x},t)=\frac{v_y(\vec{x},t)}{S_c},\ \hat{v}_z(\vec{x},t)=\frac{v_z(\vec{x},t)}{S_c}$$

$$\hat{w}_x(\vec{x},t)=\frac{w_x(\vec{x},t)}{S_w},\ \hat{w}_y(\vec{x},t)=\frac{w_y(\vec{x},t)}{S_w},\ \hat{w}_z(\vec{x},t)=\frac{w_z(\vec{x},t)}{S_w},\ \hat{P}(\vec{x},t)=\frac{P(\vec{x},t)}{S_P}$$

Finally, we redefine the memory variables so that

$$\hat{p}_r(\vec{x},t)=\frac{1}{\omega_r(\vec{x})}\,p_r(\vec{x},t)$$

This allows a slightly more computationally efficient form of the equations.

2.3.2 Finite-Difference Coefficients

The non-dimensionalized equations use the characteristic units, spatial node spacings for x, y and z dimensions, d_x, d_y, d_z , respectively, and time step, d_t , to define the finite-difference coefficients used in the numerical implementation. As stated in Section 1, we utilized fourth-order accurate spatial derivatives and second order accurate temporal derivatives. For the moving media acoustic equations, we require both staggered and non-staggered spatial derivatives.

The staggered fourth-order accurate non-dimensional finite-difference coefficients are:

$$p_i=S_c\frac{d_t}{d_i}c_{inner},\qquad q_i=S_c\frac{d_t}{d_i}c_{outer}$$

where subscript i is $x, y,$ or z , forming 6 coefficients. For Taylor Series approximates, $c_{inner}=\frac{9}{8}$ and $c_{outer}=-\frac{1}{24}$. For the non-staggered fourth-order accurate non-dimensional finite-difference coefficients we have

$$r_i=S_c\frac{2h_t}{h_i}d_{inner},\qquad s_i=S_c\frac{2h_t}{h_i}d_{outer}$$

where, again, subscript i is $x, y,$ or z , forming an additional 6 coefficients. The Taylor Series approximates are $d_{inner}=\frac{2}{3}$ and $d_{outer}=-\frac{1}{12}$. Finally, for 2-D centered interpolation of dependent variables, we utilize a 4-point formula with

$$a_{0,-1}=a_{0,0}=a_{1,-1}=a_{1,0}=\frac{1}{4}$$

2.3.3 X-Component of Particle Velocity

The non-dimensional finite-difference equations for the particle velocities are identical in the attenuative and non-attenuative cases and are

$$\hat{w}_x(x_i+\frac{d_x}{2},y_j,z_k,t_l+\frac{d_t}{2})=\hat{w}_x(x_i+\frac{d_x}{2},y_j,z_k,t_l-\frac{3d_t}{2})$$
$$-\hat{v}_x(x_i+\frac{d_x}{2},y_j,z_k)\Big\{r_x[\hat{w}_x(x_i+\frac{3d_x}{2},y_j,z_k,t_l-\frac{d_t}{2})-\hat{w}_x(x_i-\frac{d_x}{2},y_j,z_k,t_l-\frac{d_t}{2})]+$$
$$+s_x[\hat{w}_x(x_i+\frac{5d_x}{2},y_j,z_k,t_l-\frac{d_t}{2})-\hat{w}_x(x_i-\frac{3d_x}{2},y_j,z_k,t_l-\frac{d_t}{2})]\Big\}$$
$$-\hat{v}_y(x_i+\frac{d_x}{2},y_j,z_k)\Big\{r_y[\hat{w}_x(x_i+\frac{d_x}{2},y_j+d_y,z_k,t_l-\frac{d_t}{2})-\hat{w}_x(x_i+\frac{d_x}{2},y_j-d_y,z_k,t_l-\frac{d_t}{2})]+$$
$$+s_y[\hat{w}_x(x_i+\frac{d_x}{2},y_j+2d_y,z_k,t_l-\frac{d_t}{2})-\hat{w}_x(x_i+\frac{d_x}{2},y_j-2d_y,z_k,t_l-\frac{d_t}{2})]\Big\}$$
$$-\hat{v}_z(x_i+\frac{d_x}{2},y_j,z_k)\Big\{r_z[\hat{w}_x(x_i+\frac{d_x}{2},y_j,z_k+d_z,t_l-\frac{d_t}{2})-\hat{w}_x(x_i+\frac{d_x}{2},y_j,z_k-d_z,t_l-\frac{d_t}{2})]+$$
$$+s_z[\hat{w}_x(x_i+\frac{d_x}{2},y_j,z_k+2d_z,t_l-\frac{d_t}{2})-\hat{w}_x(x_i+\frac{d_x}{2},y_j,z_k-2d_z,t_l-\frac{d_t}{2})]\Big\}$$
$$-\frac{\partial\hat{v}_x}{\partial x}(x_i+\frac{d_x}{2},y_j,z_k,t_l-\frac{d_t}{2})\hat{w}_x(x_i+\frac{d_x}{2},y_j,z_k)$$
$$-\frac{\partial\hat{v}_x}{\partial y}(x_i+\frac{d_x}{2},y_j,z_k)\sum_{m=0}^{1}\sum_{n=-1}^{0}a_{mn}\hat{w}_y(x_i+m\,d_x,y_j+(n+\frac{1}{2})d_y,z_k,t_l-\frac{d_t}{2})$$
$$-\frac{\partial\hat{v}_x}{\partial z}(x_i+\frac{d_x}{2},y_j,z_k)\sum_{m=0}^{1}\sum_{n=-1}^{0}a_{mn}\hat{w}_z(x_i+m\,d_x,y_j,z_k+(n+\frac{1}{2})d_z,t_l-\frac{d_t}{2})$$
$$-\frac{1}{\hat{\rho}(x_i+\frac{d_x}{2},y_l,z_k)}\Big\{p_x\big[\hat{P}(x_i+d_x,y_j,z_k,t_l)+\hat{P}(x_i+d_x,y_j,z_k,t_l-d_t)$$
$$-\hat{P}(x_i,y_j,z_k,t_l)-\hat{P}(x_i,y_j,z_k,t_l-d_t)\big]+q_x\big[\hat{P}(x_i+2d_x,y_j,z_k,t_l)$$
$$+\hat{P}(x_i+2d_x,y_j,z_k,t_l-d_t)-\hat{P}(x_i-d_x,y_j,z_k,t_l)-\hat{P}(x_i-d_x,y_j,z_k,t_l-d_t)\big]\Big\}$$
$$+\frac{1}{\hat{\rho}(x_i+\frac{d_x}{2},y_l,z_k)}\hat{f}_x(x_i+\frac{d_x}{2},y_j,z_k,t_l-\frac{d_t}{2})$$

where the following definitions are for the shorthand notations

$$\hat{\rho}\left(x_i+\frac{d_x}{2},y_j,z_k\right)=\frac{1}{2}\left[\hat{\rho}\left(x_i,y_j,z_k\right)+\hat{\rho}\left(x_i+d_x,y_j,z_k\right)\right]$$

$$\hat{v}_x\left(x_i+\frac{d_x}{2},y_j,z_k\right)=\frac{1}{2}\left[\hat{v}_x\left(x_i,y_j,z_k\right)+\hat{v}_x\left(x_i+d_x,y_j,z_k\right)\right]$$

$$\hat{v}_y\left(x_i+\frac{d_x}{2},y_j,z_k\right)=\frac{1}{2}\left[\hat{v}_y\left(x_i,y_j,z_k\right)+\hat{v}_y\left(x_i+d_x,y_j,z_k\right)\right]$$

$$\hat{v}_z\left(x_i+\frac{d_x}{2},y_j,z_k\right)=\frac{1}{2}\left[\hat{v}_z\left(x_i,y_j,z_k\right)+\hat{v}_z\left(x_i+d_x,y_j,z_k\right)\right]$$

In addition, the spatial derivatives of the wind vectors

$$\frac{\partial\hat{v}_x}{\partial x}\left(x_i+\frac{d_x}{2},y_j,z_k\right)=\frac{2\,d_t\,S_c}{d_x}\left[\hat{v}_x\left(x_i+d_x,y_j,z_k\right)-\hat{v}_x\left(x_i,y_j,z_k\right)\right]$$

$$\frac{\partial\hat{v}_x}{\partial y}\left(x_i+\frac{d_x}{2},y_j,z_k\right)=\frac{d_t\,S_c}{2\,d_y}\left[\hat{v}_x\left(x_i+d_x,y_j+d_y,z_k\right)+\hat{v}_x\left(x_i,y_j+d_y,z_k\right)\right.$$
$$\left.-\hat{v}_x\left(x_i+d_x,y_j-d_y,z_k\right)-\hat{v}_x\left(x_i,y_j-d_y,z_k\right)\right]$$

$$\frac{\partial\hat{v}_x}{\partial z}\left(x_i+\frac{d_x}{2},y_j,z_k\right)=\frac{d_t\,S_c}{2\,d_z}\left[\hat{v}_x\left(x_i+d_x,y_j,z_k+d_z\right)+\hat{v}_x\left(x_i,y_j,z_k+d_z\right)\right.$$
$$\left.-\hat{v}_x\left(x_i+d_x,y_j,z_k-d_z\right)-\hat{v}_x\left(x_i,y_j,z_k-d_z\right)\right]$$

Lastly, the x-component of the force source vector

$$\hat{f}_x\left(x_i+\frac{d_x}{2},y_j,z_k,t_l-\frac{d_t}{2}\right)=\frac{2\,d_t\,S_c}{S_P}\,f_x\left(x_i+\frac{d_x}{2},y_j,z_k,t_l-\frac{d_t}{2}\right)$$

2.3.4 Y-Component of Particle Velocity

The non-dimensional finite-difference equations for the particle velocities are identical in the attenuative and non-attenuative cases and are

$$\hat{w}_y(x_i, y_j+\frac{d_y}{2}, z_k, t_l+\frac{d_t}{2})=\hat{w}_y(x_i, y_j+\frac{d_y}{2}, z_k, t_l-\frac{3d_t}{2})$$

$$-\hat{v}_x(x_i, y_j+\frac{d_y}{2}, z_k)\Big\{r_x[\hat{w}_y(x_i+d_x, y_j+\frac{d_y}{2}, z_k, t_l-\frac{d_t}{2})-\hat{w}_y(x_i-d_x, y_j+\frac{d_y}{2}, z_k, t_l-\frac{d_t}{2})]+$$
$$+s_x[\hat{w}_y(x_i+2d_x, y_j+\frac{d_y}{2}, z_k, t_l-\frac{d_t}{2})-\hat{w}_y(x_i-2d_x, y_j+\frac{d_y}{2}, z_k, t_l-\frac{d_t}{2})]\Big\}$$

$$-\hat{v}_y(x_i, y_j+\frac{d_y}{2}, z_k)\Big\{r_y[\hat{w}_y(x_i, y_j+\frac{3d_y}{2}, z_k, t_l-\frac{d_t}{2})-\hat{w}_y(x_i, y_j-\frac{d_y}{2}, z_k, t_l-\frac{d_t}{2})]+$$
$$+s_y[\hat{w}_y(x_i, y_j+\frac{5d_y}{2}, z_k, t_l-\frac{d_t}{2})-\hat{w}_y(x_i, y_j-\frac{3d_y}{2}, z_k, t_l-\frac{d_t}{2})]\Big\}$$

$$-\hat{v}_z(x_i, y_j+\frac{d_y}{2}, z_k)\Big\{r_z[\hat{w}_y(x_i, y_j+\frac{d_y}{2}, z_k+d_z, t_l-\frac{d_t}{2})-\hat{w}_y(x_i, y_j+\frac{d_y}{2}, z_k-d_z, t_l-\frac{d_t}{2})]+$$
$$+s_z[\hat{w}_y(x_i, y_j+\frac{d_y}{2}, z_k+2d_z, t_l-\frac{d_t}{2})-\hat{w}_y(x_i, y_j+\frac{d_y}{2}, z_k-2d_z, t_l-\frac{d_t}{2})]\Big\}$$

$$-\frac{\partial\hat{v}_y}{\partial y}(x_i, y_j+\frac{d_y}{2}, z_k, t_l-\frac{d_t}{2})\hat{w}_y(x_i, y_j+\frac{d_y}{2}, z_k)$$

$$-\frac{\partial\hat{v}_y}{\partial x}(x_i, y_j+\frac{d_y}{2}, z_k)\sum_{m=0}^{1}\sum_{n=-1}^{0}a_{mn}\hat{w}_x(x_i+(n+\frac{1}{2}), y_j+md_y, z_k, t_l-\frac{d_t}{2})$$

$$-\frac{\partial\hat{v}_y}{\partial z}(x_i, y_j+\frac{d_y}{2}, z_k)\sum_{m=0}^{1}\sum_{n=-1}^{0}a_{mn}\hat{w}_z(x_i, y_j+md_y, z_k+(n+\frac{1}{2})d_z, t_l-\frac{d_t}{2})$$

$$-\frac{1}{\hat{\rho}(x_i, y_l+\frac{d_y}{2}, z_k)}\Big\{p_x\big[\hat{P}(x_i, y_j+d_y, z_k, t_l)+\hat{P}(x_i, y_j+d_y, z_k, t_l-d_t)$$
$$-\hat{P}(x_i, y_j, z_k, t_l)-\hat{P}(x_i, y_j, z_k, t_l-d_t)\big]+q_x\big[\hat{P}(x_i, y_j+2d_y, z_k, t_l)$$
$$+\hat{P}(x_i, y_j+2d_y, z_k, t_l-d_t)-\hat{P}(x_i, y_j-d_y, z_k, t_l)-\hat{P}(x_i, y_j-d_y, z_k, t_l-d_t)\big]\Big\}$$

$$+\frac{1}{\hat{\rho}(x_i, y_l+\frac{d_y}{2}, z_k)}\hat{f}_y(x_i, y_j+\frac{d_y}{2}, z_k, t_l-\frac{d_t}{2})$$

where the following definitions are for the shorthand notations

$$\hat{\rho}(x_i, y_j+\frac{d_y}{2}, z_k)=\frac{1}{2}[\hat{\rho}(x_i, y_j, z_k)+\hat{\rho}(x_i, y_j+d_y, z_k)]$$

$$\hat{v}_x(x_i, y_j+\frac{d_y}{2}, z_k)=\frac{1}{2}[\hat{v}_x(x_i, y_j, z_k)+\hat{v}_x(x_i, y_j+d_y, z_k)]$$

$$\hat{v}_y(x_i, y_j+\frac{d_y}{2}, z_k)=\frac{1}{2}[\hat{v}_y(x_i, y_j, z_k)+\hat{v}_y(x_i, y_j+d_y, z_k)]$$

$$\hat{v}_z(x_i, y_j+\frac{d_y}{2}, z_k)=\frac{1}{2}[\hat{v}_z(x_i, y_j, z_k)+\hat{v}_z(x_i, y_j+d_y, z_k)]$$

In addition, the spatial derivatives of the wind vectors

$$\frac{\partial \hat{v}_y}{\partial y}(x_i, y_j+\frac{d_y}{2}, z_k)=\frac{2d_t S_c}{d_y}[\hat{v}_y(x_i, y_j+d_y, z_k)-\hat{v}_y(x_i, y_j, z_k)]$$

$$\frac{\partial \hat{v}_y}{\partial x}(x_i, y_j+\frac{d_y}{2}, z_k)=\frac{d_t S_c}{2d_x}\big[\hat{v}_y(x_i+d_x, y_j+d_y, z_k)+\hat{v}_y(x_i+d_x, y_j, z_k)$$
$$-\hat{v}_y(x_i-d_x, y_j+d_y, z_k)-\hat{v}_y(x_i-d_x, y_j, z_k)\big]$$

$$\frac{\partial \hat{v}_y}{\partial z}(x_i, y_j+\frac{d_y}{2}, z_k)=\frac{d_t S_c}{2d_z}\big[\hat{v}_y(x_i, y_j+d_y, z_k+d_z)+\hat{v}_y(x_i, y_j, z_k+d_z)$$
$$-\hat{v}_y(x_i, y_j+d_y, z_k-d_z)-\hat{v}_y(x_i, y_j, z_k-d_z)\big]$$

Lastly, the y-component of the force source vector

$$\hat{f}_y(x_i, y_j+\frac{d_y}{2}, z_k, t_l-\frac{d_t}{2})=\frac{2d_t S_c}{S_P} f_x(x_i, y_j+\frac{d_y}{2}, z_k, t_l-\frac{d_t}{2})$$

2.3.5 Z-Component of Particle Velocity

The non-dimensional finite-difference equations for the particle velocities are identical in the attenuative and non-attenuative cases and are

$$\hat{w}_z(x_i, y_j, z_k+\frac{d_z}{2}, t_l+\frac{d_t}{2})=\hat{w}_z(x_i, y_j, z_k+\frac{d_z}{2}, t_l-\frac{3d_t}{2})$$

$$-\hat{v}_x(x_i, y_j, z_k+\frac{d_z}{2})\Big\{r_x[\hat{w}_z(x_i+d_x, y_j, z_k+\frac{d_z}{2}, t_l-\frac{d_t}{2})-\hat{w}_z(x_i-d_x, y_j, z_k+\frac{d_z}{2}, t_l-\frac{d_t}{2})]+$$
$$+s_x[\hat{w}_z(x_i+2d_x, y_j, z_k+\frac{d_z}{2}, t_l-\frac{d_t}{2})-\hat{w}_z(x_i-2d_x, y_j, z_k+\frac{d_z}{2}, t_l-\frac{d_t}{2})]\Big\}$$

$$-\hat{v}_y(x_i, y_j, z_k+\frac{d_z}{2})\Big\{r_y[\hat{w}_z(x_i, y_j+d_y, z_k+\frac{d_z}{2}, t_l-\frac{d_t}{2})-\hat{w}_z(x_i, y_j-d_y, z_k+\frac{d_z}{2}, t_l-\frac{d_t}{2})]+$$
$$+s_y[\hat{w}_z(x_i, y_j+2d_y, z_k+\frac{d_z}{2}, t_l-\frac{d_t}{2})-\hat{w}_z(x_i, y_j-2d_y, z_k+\frac{d_z}{2}, t_l-\frac{d_t}{2})]\Big\}$$

$$-\hat{v}_z(x_i, y_j, z_k+\frac{d_z}{2})\Big\{r_z[\hat{w}_z(x_i, y_j, z_k+\frac{3d_z}{2}, t_l-\frac{d_t}{2})-\hat{w}_z(x_i, y_j, z_k-\frac{d_z}{2}, t_l-\frac{d_t}{2})]+$$
$$+s_z[\hat{w}_z(x_i, y_j, z_k+\frac{5d_z}{2}, t_l-\frac{d_t}{2})-\hat{w}_z(x_i, y_j, z_k-\frac{3d_z}{2}, t_l-\frac{d_t}{2})]\Big\}$$

$$-\frac{\partial\hat{v}_z}{\partial z}(x_i, y_j, z_k+\frac{d_z}{2}, t_l-\frac{d_t}{2})\hat{w}_z(x_i, y_j, z_k+\frac{d_z}{2})$$

$$-\frac{\partial\hat{v}_z}{\partial y}(x_i, y_j, z_k+\frac{d_z}{2})\sum_{m=0}^{1}\sum_{n=-1}^{0}a_{mn}\hat{w}_y(x_i, y_j+(n+\frac{1}{2})d_y, z_k+md_z, t_l-\frac{d_t}{2})$$

$$-\frac{\partial\hat{v}_z}{\partial x}(x_i, y_j, z_k+\frac{d_z}{2})\sum_{m=0}^{1}\sum_{n=-1}^{0}a_{mn}\hat{w}_x(x_i+(n+\frac{1}{2})d_x, y_j, z_k+md_z, t_l-\frac{d_t}{2})$$

$$-\frac{1}{\hat{\rho}(x_i, y_l, z_k+\frac{d_z}{2})}\Big\{p_x\big[\hat{P}(x_i, y_j, z_k+d_z, t_l)+\hat{P}(x_i, y_j, z_k+d_z, t_l-d_t)$$
$$-\hat{P}(x_i, y_j, z_k, t_l)-\hat{P}(x_i, y_j, z_k, t_l-d_t)\big]+q_x\big[\hat{P}(x_i, y_j, z_k+2d_z, t_l)$$
$$+\hat{P}(x_i, y_j, z_k+2d_z, t_l-d_t)-\hat{P}(x_i, y_j, z_k-d_z, t_l)-\hat{P}(x_i, y_j, z_k-d_z, t_l-d_t)\big]\Big\}$$
$$+\frac{1}{\hat{\rho}(x_i, y_l, z_k+\frac{d_z}{2})}\hat{f}_z(x_i, y_j, z_k+\frac{d_z}{2}, t_l-\frac{d_t}{2})$$

where the following definitions are for the shorthand notations

$$\hat{\rho}(x_i, y_j, z_k + \frac{d_z}{2}) = \frac{1}{2}[\hat{\rho}(x_i, y_j, z_k) + \hat{\rho}(x_i, y_j, z_k + d_z)]$$

$$\hat{v}_x(x_i, y_j, z_k + \frac{d_z}{2}) = \frac{1}{2}[\hat{v}_x(x_i, y_j, z_k) + \hat{v}_x(x_i, y_j, z_k + d_z)]$$

$$\hat{v}_y(x_i, y_j, z_k + \frac{d_z}{2}) = \frac{1}{2}[\hat{v}_y(x_i, y_j, z_k) + \hat{v}_y(x_i, y_j, z_k + d_z)]$$

$$\hat{v}_z(x_i, y_j, z_k + \frac{d_z}{2}) = \frac{1}{2}[\hat{v}_z(x_i, y_j, z_k) + \hat{v}_z(x_i, y_j, z_k + d_z)]$$

In addition, the spatial derivatives of the wind vectors

$$\frac{\partial \hat{v}_z}{\partial z}(x_i, y_j, z_k + \frac{d_z}{2}) = \frac{2 d_t S_c}{d_z}[\hat{v}_z(x_i, y_j, z_k + d_z) - \hat{v}_z(x_i, y_j, z_k)]$$

$$\frac{\partial \hat{v}_z}{\partial y}(x_i, y_j, z_k + \frac{d_z}{2}) = \frac{d_t S_c}{2 d_y}\big[\hat{v}_z(x_i, y_j + d_y, z_k + d_z) + \hat{v}_z(x_i, y_j + d_y, z_k) - \hat{v}_z(x_i, y_j - d_y, z_k + d_z) - \hat{v}_z(x_i, y_j - d_y, z_k)\big]$$

$$\frac{\partial \hat{v}_z}{\partial x}(x_i, y_j, z_k + \frac{d_z}{2}) = \frac{d_t S_c}{2 d_x}\big[\hat{v}_z(x_i + d_x, y_j, z_k + d_z) + \hat{v}_z(x_i + d_x, y_j, z_k) - \hat{v}_z(x_i - d_x, y_j, z_k + d_z) - \hat{v}_z(x_i - d_x, y_j, z_k)\big]$$

Lastly, the z-component of the force source vector

$$\hat{f}_z(x_i, y_j, z_k + \frac{d_z}{2}, t_l - \frac{d_t}{2}) = \frac{2 d_t S_c}{S_P} f_z(x_i, y_j, z_k + \frac{d_z}{2}, t_l - \frac{d_t}{2})$$

2.3.6 Pressure

The pressure updating formula contains extra terms associated with memory variables compared to the non-attenuative moving media case.

$$
\begin{aligned}
\hat{P}(x_i, y_j, z_k, t_l + d_t) = {} & \hat{P}(x_i, y_j, z_k, t_l) \\
& - \hat{v}_x(x_i, y_j, z_k)\{r_x[\hat{P}(x_i + d_x, y_j, z_k, t_l) - \hat{P}(x_i - d_x, y_j, z_k, t_l)] \\
& \quad + s_x[\hat{P}(x_i + 2d_x, y_j, z_k, t_l) - \hat{P}(x_i - 2d_x, y_j, z_k, t_l)]\} \\
& - \hat{v}_y(x_i, y_j, z_k)\{r_y[\hat{P}(x_i, y_j + d_y, z_k, t_l) - \hat{P}(x_i, y_j - d_y, z_k, t_l)] \\
& \quad + s_y[\hat{P}(x_i, y_j + 2d_y, z_k, t_l) - \hat{P}(x_i, y_j - 2d_y, z_k, t_l)]\} \\
& - \hat{v}_z(x_i, y_j, z_k)\{r_z[\hat{P}(x_i, y_j, z_k + d_z, t_l) - \hat{P}(x_i, y_j, z_k - d_z, t_l)] \\
& \quad + s_z[\hat{P}(x_i, y_j, z_k + 2d_z, t_l) - \hat{P}(x_i, y_j, z_k - 2d_z, t_l)]\} \\
& - \hat{\kappa}(x_i, y_j, z_k)\Bigg\{ p_x\Bigg[\hat{w}_x(x_i + \frac{d_x}{2}, y_j, z_k, t_l + \frac{d_t}{2}) + \hat{w}_x(x_i + \frac{d_x}{2}, y_j, z_k, t_l - \frac{d_t}{2}) \\
& \quad - \hat{w}_x(x_i - \frac{d_x}{2}, y_j, z_k, t_l + \frac{d_t}{2}) - \hat{w}_x(x_i - \frac{d_x}{2}, y_j, z_k, t_l - \frac{d_t}{2})\Bigg] \\
& \quad + q_x\Bigg[\hat{w}_x(x_i + \frac{3d_x}{2}, y_j, z_k, t_l + \frac{d_t}{2}) + \hat{w}_x(x_i + \frac{3d_x}{2}, y_j, z_k, t_l - \frac{d_t}{2}) \\
& \quad - \hat{w}_x(x_i - \frac{3d_x}{2}, y_j, z_k, t_l + \frac{d_t}{2}) - \hat{w}_x(x_i - \frac{3d_x}{2}, y_j, z_k, t_l - \frac{d_t}{2})\Bigg] \\
& \quad p_y\Bigg[\hat{w}_y(x_i, y_j + \frac{d_y}{2}, z_k, t_l + \frac{d_t}{2}) + \hat{w}_y(x_i, y_j + \frac{d_y}{2}, z_k, t_l - \frac{d_t}{2}) \\
& \quad - \hat{w}_y(x_i, y_j - \frac{d_y}{2}, z_k, t_l + \frac{d_t}{2}) - \hat{w}_y(x_i, y_j - \frac{d_y}{2}, z_k, t_l - \frac{d_t}{2})\Bigg] \\
& \quad + q_y\Bigg[\hat{w}_y(x_i, y_j + \frac{3d_y}{2}, z_k, t_l + \frac{d_t}{2}) + \hat{w}_y(x_i, y_j + \frac{3d_y}{2}, z_k, t_l - \frac{d_t}{2}) \\
& \quad - \hat{w}_y(x_i, y_j - \frac{3d_y}{2}, z_k, t_l + \frac{d_t}{2}) - \hat{w}_y(x_i, y_j - \frac{3d_y}{2}, z_k, t_l - \frac{d_t}{2})\Bigg] \\
& \quad + p_z\Bigg[\hat{w}_z(x_i, y_j, z_k + \frac{d_z}{2}, t_l + \frac{d_t}{2}) + \hat{w}_z(x_i, y_j, z_k + \frac{d_z}{2}, t_l - \frac{d_t}{2}) \\
& \quad - \hat{w}_z(x_i, y_j, z_k - \frac{d_z}{2}, t_l + \frac{d_t}{2}) - \hat{w}_z(x_i, y_j, z_k - \frac{d_x}{2}, t_l - \frac{d_t}{2})\Bigg] \\
& \quad + q_z\Bigg[\hat{w}_z(x_i, y_j, z_k + \frac{3d_z}{2}, t_l + \frac{d_t}{2}) + \hat{w}_z(x_i, y_j, z_k + \frac{3d_z}{2}, t_l - \frac{d_t}{2}) \\
& \quad - \hat{w}_z(x_i, y_j, z_k - \frac{3d_z}{2}, t_l + \frac{d_t}{2}) - \hat{w}_z(x_i, y_j, z_k - \frac{3d_z}{2}, t_l - \frac{d_t}{2})\Bigg]\Bigg\} \\
& - \hat{\kappa}(x_i, y_j, z_k)\sum_{r=1}^{R}\frac{1}{2}d_t\omega_r[\hat{p}_r(x_i, y_j, z_k, t_l + d_t) + \hat{p}_r(x_i, y_j, z_k, t_l)] \\
& + \hat{e}(x_i, y_j, z_k, t_l + d_t) - \hat{e}(x_i, y_j, z_k, t_l)
\end{aligned}
$$

Since all material parameters including wind vector components are on the same raster as pressure, no averaging of these quantities is required.

2.3.7 Memory Variables

There are R memory variable equations, each with the same form. The r^{th} memory variable equation is

$$\hat{p}_r(x_i, y_j, z_k, t_l + d_t) = \frac{2 - d_t \omega_r}{2 + d_t \omega_r} \hat{p}_r(x_i, y_j, z_k, t_l)$$
$$- \frac{2 a_r}{2 + d_t \omega_r} \Bigg\{ p_x \Bigg[\hat{w}_x(x_i + \frac{d_x}{2}, y_j, z_k, t_l + \frac{d_t}{2}) + \hat{w}_x(x_i + \frac{d_x}{2}, y_j, z_k, t_l - \frac{d_t}{2})$$
$$- \hat{w}_x(x_i - \frac{d_x}{2}, y_j, z_k, t_l + \frac{d_t}{2}) - \hat{w}_x(x_i - \frac{d_x}{2}, y_j, z_k, t_l - \frac{d_t}{2}) \Bigg]$$
$$+ q_x \Bigg[\hat{w}_x(x_i + \frac{3 d_x}{2}, y_j, z_k, t_l + \frac{d_t}{2}) + \hat{w}_x(x_i + \frac{3 d_x}{2}, y_j, z_k, t_l - \frac{d_t}{2})$$
$$- \hat{w}_x(x_i - \frac{3 d_x}{2}, y_j, z_k, t_l + \frac{d_t}{2}) - \hat{w}_x(x_i - \frac{3 d_x}{2}, y_j, z_k, t_l - \frac{d_t}{2}) \Bigg]$$
$$p_y \Bigg[\hat{w}_y(x_i, y_j + \frac{d_y}{2}, z_k, t_l + \frac{d_t}{2}) + \hat{w}_y(x_i, y_j + \frac{d_y}{2}, z_k, t_l - \frac{d_t}{2})$$
$$- \hat{w}_y(x_i, y_j - \frac{d_y}{2}, z_k, t_l + \frac{d_t}{2}) - \hat{w}_y(x_i, y_j - \frac{d_y}{2}, z_k, t_l - \frac{d_t}{2}) \Bigg]$$
$$+ q_y \Bigg[\hat{w}_y(x_i, y_j + \frac{3 d_y}{2}, z_k, t_l + \frac{d_t}{2}) + \hat{w}_y(x_i, y_j + \frac{3 d_y}{2}, z_k, t_l - \frac{d_t}{2})$$
$$- \hat{w}_y(x_i, y_j - \frac{3 d_y}{2}, z_k, t_l + \frac{d_t}{2}) - \hat{w}_y(x_i, y_j - \frac{3 d_y}{2}, z_k, t_l - \frac{d_t}{2}) \Bigg]$$
$$+ p_z \Bigg[\hat{w}_z(x_i, y_j, z_k + \frac{d_z}{2}, t_l + \frac{d_t}{2}) + \hat{w}_z(x_i, y_j, z_k + \frac{d_z}{2}, t_l - \frac{d_t}{2})$$
$$- \hat{w}_z(x_i, y_j, z_k - \frac{d_z}{2}, t_l + \frac{d_t}{2}) - \hat{w}_z(x_i, y_j, z_k - \frac{d_x}{2}, t_l - \frac{d_t}{2}) \Bigg]$$
$$+ q_z \Bigg[\hat{w}_z(x_i, y_j, z_k + \frac{3 d_z}{2}, t_l + \frac{d_t}{2}) + \hat{w}_z(x_i, y_j, z_k + \frac{3 d_z}{2}, t_l - \frac{d_t}{2})$$
$$- \hat{w}_z(x_i, y_j, z_k - \frac{3 d_z}{2}, t_l + \frac{d_t}{2}) - \hat{w}_z(x_i, y_j, z_k - \frac{3 d_z}{2}, t_l - \frac{d_t}{2}) \Bigg] \Bigg\}$$

2.3.8 Numerical Efficiency

Cache coherency is important for computational efficiency. Since each (x_i, y_j, z_k) grid point is associated with one of N_m attenuation models, the R ω_r and a_r coefficients associated with that grid point must be efficiently loaded in order to avoid double index dereferencing,

which with C/C++ is relatively slow. To maximize cache efficiency, the pressure and memory variable updating is done in stages. In the first stage the parameters for the first attenuation mechanism, ω_0 and a_0 , are copied to a temporary 1-D array for all x_i for a fixed y_j, z_k . Then the non-attenuative portions of the pressure updating equations are computed concurrently with updating the first memory variable, $\hat{p}_0$, which is then added to the non-attenuative portion of the pressure. Finally, each remaining R-1 mechanisms is loaded sequentially into the 1-D array, the corresponding memory variable updated, and added to the pressure. In tests this method provided a 2.5 x speedup over updating in the order that the equations as written may suggest.

3. ABSORBING BOUNDARY CONDITIONS

3.1 Introduction

It is more efficient in most cases to limit the simulation domain spatially for both computational and practical reasons. However, if the computational domain were simply truncated at the edges of spatial domain of interest, strong reflections of waves would occur that would not be naturally present. This will greatly contaminate the simulations, especially in later time, and are undesirable. To mitigate against these domain boundary reflections, absorbing boundary conditions (ABC) are established, which as their name implies, greatly reduce the incoming and reflected outgoing waves impinging on a domain boundary. Several different types of absorbing boundary conditions have been proposed, with one of the simplest being the so-called wavefield taper, or sponge, boundary conditions (Cerjan et al., 1985). Although simple to implement, these boundary conditions typically require relatively thick zones around the domain boundaries to be effective and have poor grazing incidence performance. Another popular absorbing boundary condition is the perfectly matched layer (PML) boundary condition introduced by Beringer (1994). These boundary conditions in theory are perfect (meaning no reflection at the interface between the interior and absorbing boundary condition layer), but in practice do have a small reflection at this interface. The PML allows much thinner ABC layer thicknesses and much smaller overall reflection amplitudes relative to the wavefield taper zones. Again, however, PMLs perform poorly for grazing incidence waves on the boundary layer. To combat this, a variant of the PML, called the convolutional PML (CPML) was introduced (Komatitsch and Martin, 2007). Although this does perform better at grazing incidence, it only delays the poor performance to somewhat larger angles of incidence, often producing interface waves that remain trapped in the ABC layer and which emanate energy back into the interior at near-grazing incidence. A second problem, with both PMLs and CPMLs, is that they are known to be unstable in certain anisotropic media. One solution to both of the above issues is the so-called multiple PML (MPML) (Meza-Fajardo and Papageorgiou, 2008). Both PMLs and CPMLs only damp the wavefield in the direction perpendicular to domain boundary and do not damp the wavefield at all for motion parallel to the boundary. This is actually what allows, in theory, the perfect reflectionless interface between the interior and PML layer. However, it also allows for interface waves to develop that propagate parallel to the boundary and build up instead of attenuate. The MPML introduces a small attenuation for motion parallel to the boundary called the cross-factor. Use of the cross-factor does destroy the "perfectness" of the interior-PML interface, but it does greatly reduce, and in many cases eliminate, interface waves and instabilities caused by anisotropy. Typically cross-factors of 1-5% of the the perpendicular absorption is sufficient to practically eliminate these undesirable effects. The original PML is a special case of a CPML, which itself is a special case of an MPML. Thus, in TDAAPS the MPML is the only PML-type ABC that is implemented internally, with requests for a PML or CPML just setting the appropriate parameters of the MPML to produce the desired PML-type. This does increase computational effort but for a CPML it amounts to about 5% slowdown relative to using special code for a CPML only.

3.2 MPML Implementation

Similar to physical attenuation described in Chapter 2, implementation of an MPML utilizes memory variables. However, unlike physical attenuation, an MPML applies memory variables in all dependent variables update equations (pressure and the three components of velocity). There are a total of 15 MPML memory variables and equations that augment the system provided in Chapter 2 that must be solved in the ABC layers. One needs at least one MPML memory variable for each derivative direction per update variable, which accounts for 9 of the

memory variables for the updates of the 3 components of velocity. For the pressure updating, however, there are 6 memory variables. This is due to the fact that physical attenuation only depends on the divergence of the velocity vector; thus, 3 memory variables are needed just for the 3 divergence terms. The remainder of the pressure updating equations also have spatial derivatives and thus requires 3 separate memory variables.

3.2.1 MPML Parameters

The MPML implemented in TDAAPS is parameterized by 4 factors: the MPML width (w), the theoretical reflection percentage desired at the domain boundary (R), a "cutoff" frequency (α), and the cross-factor (χ). The MPML width is the thickness of the ABC layer from each domain boundary in nodes, with 10 being a typical number. The theoretical reflection percentage is not directly linked to the actual reflection coefficient, since making this too small, can actually increase reflections in practice due to there being too sharp an onset to the layer at the interior-PML interface. The best value for this varies somewhat, but it tends not to be overly sensitive to this parameter, but a value of 0.001% tends to work well in many instances. The "cutoff" frequency is really a cutoff between behaving more like an original PML above this frequency and tapering to less attenuation below this frequency (introduced in the CPML and has a value of 0 for a pure PML). A value of πf_{peak} where f_{peak} is near the peak of the spectrum expected in the far field is recommended. Finally, the MPML cross-factor, which as described above gives the fractional amount of attenuation in the direction parallel to the boundary relative to perpendicular to it. A pure CPML and PML have the cross-factor as 0, but typically values of 0.01 to 0.05 work in most instances. Internally the above parameters are converted to values that are actually used in the algorithm. The PML attenuation factor, σ , is defined as

$$\sigma_{max} = \frac{-1.5 \log(R) v_{max}}{w d_h}$$

where v_{max} is the maximum wavespeed in the current model and d_h is the node spacing. Another parameter that affects performance of all PMLs is the shape of the taper that goes from the PML-interior interface to the domain boundary. In TDAAPS, a quadratic that varies from 0 at the PML-interior interface to σ_{max} at the domain boundary is used. For CPMLs, one also needs a taper function for α . In TDAAPS, we use a linear function that actually has a value of α at the interior-PML interface and goes to 0 at the domain boundary. The cross-factor is constant throughout the PML layer. Once these parameters are given two functions are defined that simplify computations

$$b\perp(x_i, y_j, z_k) = \exp(-2\, dt(\sigma(x_i, y_j, z_k) + \alpha(x_i, y_j, z_k)))$$

$$a\perp(x_i, y_j, z_k) = \sigma(x_i, y_j, z_k) \frac{(b(x_i, y_j, z_k) - 1)}{(\sigma(x_i, y_j, z_k) + \alpha(x_i, y_j, z_k))}$$

for perpendicular attenuation. For the MPML, when χ is non-zero, the parallel directions are defined by

$$b\|(x_i, y_j, z_k) = \exp(-2\chi\, dt\, \sigma(x_i, y_j, z_k))$$

$$a\|(x_i, y_j, z_k) = b\|(x_i, y_j, z_k) - 1$$

It is important to note that these functions of space must be defined, as appropriate, for whole and half-integer locations. Also, within edge and corner layers, two or three PML layers are combined. For example, at an X-Y edge, the PML layer for a purely X layer is combined with a purely Y layer.

The memory variable updating equations are the same in each case. For memory variable g_r where r is one of the 15 memory variables

$$g_r(x_i, y_j, z_k, t_l + d_t) = b(x_i, y_j, z_k) g_r(x_i, y_j, z_k, t_l) + a(x_i, y_j, z_k) D_r(x_i, y_j, z_k, t_l + d_t/2)$$
$$= G(g_r, D_r)$$

where b and a are parameters of the MPML defined above as either the parallel or perpendicular variety, and are functions of space only, and D_r is a term that depends on a sum of terms that contain a derivative of space in a certain direction.

The following are rearrangements of the equations given in Chapter 2 with the addition of the MPML. Note that for simplicity the source terms are not included in the equations below, but are added in the same manner as given in Chapter 2, i.e., they are not affected by the MPML. However, in practice, source terms should not be placed within the PML layer. All terms have the same definitions as given in Chapter 2 if not provided here.

3.2.2 X-Component of Particle Velocity

$$D_{vxx} = -\hat{v}_x\left(x_i + \frac{d_x}{2}, y_j, z_k\right)\Bigg\{ r_x\left[\hat{w}_x\left(x_i + \frac{3d_x}{2}, y_j, z_k, t_l - \frac{d_t}{2}\right) - \hat{w}_x\left(x_i - \frac{d_x}{2}, y_j, z_k, t_l - \frac{d_t}{2}\right)\right] +$$
$$+ s_x\left[\hat{w}_x\left(x_i + \frac{5d_x}{2}, y_j, z_k, t_l - \frac{d_t}{2}\right) - \hat{w}_x\left(x_i - \frac{3d_x}{2}, y_j, z_k, t_l - \frac{d_t}{2}\right)\right]\Bigg\}$$
$$- \frac{\partial \hat{v}_x}{\partial x}\left(x_i + \frac{d_x}{2}, y_j, z_k, t_l - \frac{d_t}{2}\right) \hat{w}_x\left(x_i + \frac{d_x}{2}, y_j, z_k\right)$$
$$- \frac{1}{\hat{\rho}\left(x_i + \frac{d_x}{2}, y_l, z_k\right)}\Big\{ p_x\Big[\hat{P}(x_i + d_x, y_j, z_k, t_l) + \hat{P}(x_i + d_x, y_j, z_k, t_l - d_t)$$
$$- \hat{P}(x_i, y_j, z_k, t_l) - \hat{P}(x_i, y_j, z_k, t_l - d_t)\Big] + q_x\Big[\hat{P}(x_i + 2d_x, y_j, z_k, t_l)$$
$$+ \hat{P}(x_i + 2d_x, y_j, z_k, t_l - d_t) - \hat{P}(x_i - d_x, y_j, z_k, t_l) - \hat{P}(x_i - d_x, y_j, z_k, t_l - d_t)\Big]\Big\}$$
$$D_{vxy} = -\hat{v}_y\left(x_i + \frac{d_x}{2}, y_j, z_k\right)\Bigg\{ r_y\left[\hat{w}_x\left(x_i + \frac{d_x}{2}, y_j + d_y, z_k, t_l - \frac{d_t}{2}\right) - \hat{w}_x\left(x_i + \frac{d_x}{2}, y_j - d_y, z_k, t_l - \frac{d_t}{2}\right)\right] +$$
$$+ s_y\left[\hat{w}_x\left(x_i + \frac{d_x}{2}, y_j + 2d_y, z_k, t_l - \frac{d_t}{2}\right) - \hat{w}_x\left(x_i + \frac{d_x}{2}, y_j - 2d_y, z_k, t_l - \frac{d_t}{2}\right)\right]\Bigg\}$$
$$- \frac{\partial \hat{v}_x}{\partial y}\left(x_i + \frac{d_x}{2}, y_j, z_k\right) \sum_{m=0}^{1} \sum_{n=-1}^{0} a_{mn} \hat{w}_y\left(x_i + m d_x, y_j + \left(n + \frac{1}{2}\right) d_y, z_k, t_l - \frac{d_t}{2}\right)$$

$$D_{vxz}=-\hat{v}_z(x_i+\frac{d_x}{2},y_j,z_k)\Big\{r_z[\hat{w}_x(x_i+\frac{d_x}{2},y_j,z_k+d_z,t_l-\frac{d_t}{2})-\hat{w}_x(x_i+\frac{d_x}{2},y_j,z_k-d_z,t_l-\frac{d_t}{2})]+$$
$$+s_z[\hat{w}_x(x_i+\frac{d_x}{2},y_j,z_k+2d_z,t_l-\frac{d_t}{2})-\hat{w}_x(x_i+\frac{d_x}{2},y_j,z_k-2d_z,t_l-\frac{d_t}{2})]\Big\}$$
$$-\frac{\partial\hat{v}_x}{\partial z}(x_i+\frac{d_x}{2},y_j,z_k)\sum_{m=0}^{1}\sum_{n=-1}^{0}a_{mn}\hat{w}_z(x_i+md_x,y_j,z_k+(n+\frac{1}{2})d_z,t_l-\frac{d_t}{2})$$
$$g_{vxx}=G(g_{vxx},D_{vxx})$$
$$g_{vxy}=G(g_{vxy},D_{vxy})$$
$$g_{vxz}=G(g_{vxz},D_{vxz})$$
$$\hat{w}_x(x_i+\frac{d_x}{2},y_j,z_k,t_l+\frac{d_t}{2})=\hat{w}_x(x_i+\frac{d_x}{2},y_j,z_k,t_l-\frac{3d_t}{2})+D_{vxx}+D_{vxy}+D_{vxz}+g_{vxx}+g_{vxy}+g_{vxz}$$

3.2.3 Y-Component of Particle Velocity

$$D_{vyx}=-\hat{v}_x(x_i,y_j+\frac{d_y}{2},z_k)\Big\{r_x[\hat{w}_y(x_i+d_x,y_j+\frac{d_y}{2},z_k,t_l-\frac{d_t}{2})-\hat{w}_y(x_i-d_x,y_j+\frac{d_y}{2},z_k,t_l-\frac{d_t}{2})]+$$
$$+s_x[\hat{w}_y(x_i+2d_x,y_j+\frac{d_y}{2},z_k,t_l-\frac{d_t}{2})-\hat{w}_y(x_i-2d_x,y_j+\frac{d_y}{2},z_k,t_l-\frac{d_t}{2})]\Big\}$$
$$-\frac{\partial\hat{v}_y}{\partial x}(x_i,y_j+\frac{d_y}{2},z_k)\sum_{m=0}^{1}\sum_{n=-1}^{0}a_{mn}\hat{w}_x(x_i+(n+\frac{1}{2}),y_j+md_y,z_k,t_l-\frac{d_t}{2})$$
$$D_{vyy}=-\hat{v}_y(x_i,y_j+\frac{d_y}{2},z_k)\Big\{r_y[\hat{w}_y(x_i,y_j+\frac{3d_y}{2},z_k,t_l-\frac{d_t}{2})-\hat{w}_y(x_i,y_j-\frac{d_y}{2},z_k,t_l-\frac{d_t}{2})]+$$
$$+s_y[\hat{w}_y(x_i,y_j+\frac{5d_y}{2},z_k,t_l-\frac{d_t}{2})-\hat{w}_y(x_i,y_j-\frac{3d_y}{2},z_k,t_l-\frac{d_t}{2})]\Big\}$$
$$-\frac{\partial\hat{v}_y}{\partial y}(x_i,y_j+\frac{d_y}{2},z_k,t_l-\frac{d_t}{2})\hat{w}_y(x_i,y_j+\frac{d_y}{2},z_k)$$
$$-\frac{1}{\hat{\rho}(x_i,y_l+\frac{d_y}{2},z_k)}\Big\{p_x\big[\hat{P}(x_i,y_j+d_y,z_k,t_l)+\hat{P}(x_i,y_j+d_y,z_k,t_l-d_t)$$
$$-\hat{P}(x_i,y_j,z_k,t_l)-\hat{P}(x_i,y_j,z_k,t_l-d_t)\big]+q_x\big[\hat{P}(x_i,y_j+2d_y,z_k,t_l)$$
$$+\hat{P}(x_i,y_j+2d_y,z_k,t_l-d_t)-\hat{P}(x_i,y_j-d_y,z_k,t_l)-\hat{P}(x_i,y_j-d_y,z_k,t_l-d_t)\big]\Big\}$$
$$D_{vyz}=-\hat{v}_z(x_i,y_j+\frac{d_y}{2},z_k)\Big\{r_z[\hat{w}_y(x_i,y_j+\frac{d_y}{2},z_k+d_z,t_l-\frac{d_t}{2})-\hat{w}_y(x_i,y_j+\frac{d_y}{2},z_k-d_z,t_l-\frac{d_t}{2})]+$$
$$+s_z[\hat{w}_y(x_i,y_j+\frac{d_y}{2},z_k+2d_z,t_l-\frac{d_t}{2})-\hat{w}_y(x_i,y_j+\frac{d_y}{2},z_k-2d_z,t_l-\frac{d_t}{2})]\Big\}$$
$$-\frac{\partial\hat{v}_y}{\partial z}(x_i,y_j+\frac{d_y}{2},z_k)\sum_{m=0}^{1}\sum_{n=-1}^{0}a_{mn}\hat{w}_z(x_i,y_j+md_y,z_k+(n+\frac{1}{2})d_z,t_l-\frac{d_t}{2})$$

$$g_{vyx}=G\left(g_{vyx},D_{vyx}\right)$$
$$g_{vyy}=G\left(g_{vyy},D_{vyy}\right)$$
$$g_{vyz}=G\left(g_{vyz},D_{vyz}\right)$$
$$\hat{w}_y\left(x_i,y_j+\frac{d_y}{2},z_k,t_l+\frac{d_t}{2}\right)=\hat{w}_y\left(x_i,y_j+\frac{d_y}{2},z_k,t_l-\frac{3d_t}{2}\right)+D_{vyx}+D_{vyy}+D_{vyz}+g_{vyx}+g_{vyy}+g_{vyz}$$

3.2.4 Z-Component of Particle Velocity

$$D_{vzx}=-\hat{v}_x\left(x_i,y_j,z_k+\frac{d_z}{2}\right)\Bigg\{r_x\left[\hat{w}_z\left(x_i+d_x,y_j,z_k+\frac{d_z}{2},t_l-\frac{d_t}{2}\right)-\hat{w}_z\left(x_i-d_x,y_j,z_k+\frac{d_z}{2},t_l-\frac{d_t}{2}\right)\right]+$$
$$+s_x\left[\hat{w}_z\left(x_i+2d_x,y_j,z_k+\frac{d_z}{2},t_l-\frac{d_t}{2}\right)-\hat{w}_z\left(x_i-2d_x,y_j,z_k+\frac{d_z}{2},t_l-\frac{d_t}{2}\right)\right]\Bigg\}$$
$$-\frac{\partial\hat{v}_z}{\partial x}\left(x_i,y_j,z_k+\frac{d_z}{2}\right)\sum_{m=0}^{1}\sum_{n=-1}^{0}a_{mn}\hat{w}_x\left(x_i+\left(n+\frac{1}{2}\right)d_x,y_j,z_k+md_z,t_l-\frac{d_t}{2}\right)$$
$$D_{vzy}=-\hat{v}_y\left(x_i,y_j,z_k+\frac{d_z}{2}\right)\Bigg\{r_y\left[\hat{w}_z\left(x_i,y_j+d_y,z_k+\frac{d_z}{2},t_l-\frac{d_t}{2}\right)-\hat{w}_z\left(x_i,y_j-d_y,z_k+\frac{d_z}{2},t_l-\frac{d_t}{2}\right)\right]+$$
$$+s_y\left[\hat{w}_z\left(x_i,y_j+2d_y,z_k+\frac{d_z}{2},t_l-\frac{d_t}{2}\right)-\hat{w}_z\left(x_i,y_j-2d_y,z_k+\frac{d_z}{2},t_l-\frac{d_t}{2}\right)\right]\Bigg\}$$
$$-\frac{\partial\hat{v}_z}{\partial y}\left(x_i,y_j,z_k+\frac{d_z}{2}\right)\sum_{m=0}^{1}\sum_{n=-1}^{0}a_{mn}\hat{w}_y\left(x_i,y_j+\left(n+\frac{1}{2}\right)d_y,z_k+md_z,t_l-\frac{d_t}{2}\right)$$
$$D_{vzz}=-\hat{v}_z\left(x_i,y_j,z_k+\frac{d_z}{2}\right)\Bigg\{r_z\left[\hat{w}_z\left(x_i,y_j,z_k+\frac{3d_z}{2},t_l-\frac{d_t}{2}\right)-\hat{w}_z\left(x_i,y_j,z_k-\frac{d_z}{2},t_l-\frac{d_t}{2}\right)\right]+$$
$$+s_z\left[\hat{w}_z\left(x_i,y_j,z_k+\frac{5d_z}{2},t_l-\frac{d_t}{2}\right)-\hat{w}_z\left(x_i,y_j,z_k-\frac{3d_z}{2},t_l-\frac{d_t}{2}\right)\right]\Bigg\}$$
$$-\frac{\partial\hat{v}_z}{\partial z}\left(x_i,y_j,z_k+\frac{d_z}{2},t_l-\frac{d_t}{2}\right)\hat{w}_z\left(x_i,y_j,z_k+\frac{d_z}{2}\right)$$
$$-\frac{1}{\hat{\rho}\left(x_i,y_l,z_k+\frac{d_z}{2}\right)}\Bigg\{p_x\Big[\hat{P}\left(x_i,y_j,z_k+d_z,t_l\right)+\hat{P}\left(x_i,y_j,z_k+d_z,t_l-d_t\right)$$
$$-\hat{P}\left(x_i,y_j,z_k,t_l\right)-\hat{P}\left(x_i,y_j,z_k,t_l-d_t\right)\Big]+q_x\Big[\hat{P}\left(x_i,y_j,z_k+2d_z,t_l\right)$$
$$+\hat{P}\left(x_i,y_j,z_k+2d_z,t_l-d_t\right)-\hat{P}\left(x_i,y_j,z_k-d_z,t_l\right)-\hat{P}\left(x_i,y_j,z_k-d_z,t_l-d_t\right)\Big]\Bigg\}$$
$$g_{vzx}=G\left(g_{vzx},D_{vzx}\right)$$
$$g_{vzy}=G\left(g_{vzy},D_{vzy}\right)$$
$$g_{vzz}=G\left(g_{vzz},D_{vzz}\right)$$
$$\hat{w}_z\left(x_i,y_j,z_k+\frac{d_z}{2},t_l+\frac{d_t}{2}\right)=\hat{w}_z\left(x_i,y_j,z_k+\frac{d_z}{2},t_l-\frac{3d_t}{2}\right)+D_{vzx}+D_{vzy}+D_{vzz}+g_{vzx}+g_{vzy}+g_{vzz}$$

3.2.5 Physical Memory Variables

The physical memory variables (akin to Section 2.3.7) are changed within an MPML.

$$D_{mx}=p_x\Big[\hat{w}_x(x_i+\frac{d_x}{2},y_j,z_k,t_l+\frac{d_t}{2})+\hat{w}_x(x_i+\frac{d_x}{2},y_j,z_k,t_l-\frac{d_t}{2})$$
$$-\hat{w}_x(x_i-\frac{d_x}{2},y_j,z_k,t_l+\frac{d_t}{2})-\hat{w}_x(x_i-\frac{d_x}{2},y_j,z_k,t_l-\frac{d_t}{2})\Big]$$
$$+q_x\Big[\hat{w}_x(x_i+\frac{3d_x}{2},y_j,z_k,t_l+\frac{d_t}{2})+\hat{w}_x(x_i+\frac{3d_x}{2},y_j,z_k,t_l-\frac{d_t}{2})$$
$$-\hat{w}_x(x_i-\frac{3d_x}{2},y_j,z_k,t_l+\frac{d_t}{2})-\hat{w}_x(x_i-\frac{3d_x}{2},y_j,z_k,t_l-\frac{d_t}{2})\Big]$$
$$D_{my}=p_y\Big[\hat{w}_y(x_i,y_j+\frac{d_y}{2},z_k,t_l+\frac{d_t}{2})+\hat{w}_y(x_i,y_j+\frac{d_y}{2},z_k,t_l-\frac{d_t}{2})$$
$$-\hat{w}_y(x_i,y_j-\frac{d_y}{2},z_k,t_l+\frac{d_t}{2})-\hat{w}_y(x_i,y_j-\frac{d_y}{2},z_k,t_l-\frac{d_t}{2})\Big]$$
$$+q_y\Big[\hat{w}_y(x_i,y_j+\frac{3d_y}{2},z_k,t_l+\frac{d_t}{2})+\hat{w}_y(x_i,y_j+\frac{3d_y}{2},z_k,t_l-\frac{d_t}{2})$$
$$-\hat{w}_y(x_i,y_j-\frac{3d_y}{2},z_k,t_l+\frac{d_t}{2})-\hat{w}_y(x_i,y_j-\frac{3d_y}{2},z_k,t_l-\frac{d_t}{2})\Big]$$
$$D_{mz}=p_z\Big[\hat{w}_z(x_i,y_j,z_k+\frac{d_z}{2},t_l+\frac{d_t}{2})+\hat{w}_z(x_i,y_j,z_k+\frac{d_z}{2},t_l-\frac{d_t}{2})$$
$$-\hat{w}_z(x_i,y_j,z_k-\frac{d_z}{2},t_l+\frac{d_t}{2})-\hat{w}_z(x_i,y_j,z_k-\frac{d_x}{2},t_l-\frac{d_t}{2})\Big]$$
$$+q_z\Big[\hat{w}_z(x_i,y_j,z_k+\frac{3d_z}{2},t_l+\frac{d_t}{2})+\hat{w}_z(x_i,y_j,z_k+\frac{3d_z}{2},t_l-\frac{d_t}{2})$$
$$-\hat{w}_z(x_i,y_j,z_k-\frac{3d_z}{2},t_l+\frac{d_t}{2})-\hat{w}_z(x_i,y_j,z_k-\frac{3d_z}{2},t_l-\frac{d_t}{2})\Big]$$

$$g_{mx}=G(g_{mx},D_{mx})$$
$$g_{my}=G(g_{my},D_{my})$$
$$g_{mz}=G(g_{mz},D_{mz})$$
$$\hat{p}_r(x_i,y_j,z_k,t_l+d_t)=\frac{2-d_t\omega_r}{2+d_t\omega_r}\hat{p}_r(x_i,y_j,z_k,t_l)$$
$$-\frac{2a_r}{2+d_t\omega_r}\{D_{mx}+D_{my}+D_{mz}+g_{mx}+g_{my}+g_{mz}\}$$

3.2.6 Pressure

$$D_{px}=-\hat{v_x}(x_i,y_j,z_k)\{r_x[\hat{P}(x_i+d_x,y_j,z_k,t_l)-\hat{P}(x_i-d_x,y_j,z_k,t_l)]$$
$$+s_x[\hat{P}(x_i+2d_x,y_j,z_k,t_l)-\hat{P}(x_i-2d_x,y_j,z_k,t_l)]\}$$

$$D_{py}=-\hat{v}_y(x_i,y_j,z_k)\left\{r_y[\hat{P}(x_i,y_j+d_y,z_k,t_l)-\hat{P}(x_i,y_j-d_y,z_k,t_l)]\right.$$
$$\left.+s_y[\hat{P}(x_i,y_j+2d_y,z_k,t_l)-\hat{P}(x_i,y_j-2d_y,z_k,t_l)]\right\}$$
$$D_{pz}=-\hat{v}_z(x_i,y_j,z_k)\left\{r_z[\hat{P}(x_i,y_j,z_k+d_z,t_l)-\hat{P}(x_i,y_j,z_k-d_z,t_l)]\right.$$
$$\left.+s_z[\hat{P}(x_i,y_j,z_k+2d_z,t_l)-\hat{P}(x_i,y_j,z_k-2d_z,t_l)]\right\}$$
$$g_{px}=G(g_{px},D_{px})$$
$$g_{py}=G(g_{py},D_{py})$$
$$g_{pz}=G(g_{pz},D_{pz})$$
$$\hat{P}(x_i,y_j,z_k,t_l+d_t)=\hat{P}(x_i,y_j,z_k,t_l)+D_{px}+D_{py}+D_{pz}$$
$$-\hat{\kappa}(x_i,y_j,z_k)\left[D_{mx}+D_{my}+D_{mz}+g_{mx}+g_{my}+g_{mz}\right]+g_{px}+g_{py}+g_{pz}$$
$$-\hat{\kappa}(x_i,y_j,z_k)\sum_{r=1}^{R}\frac{1}{2}d_t\omega_r[\hat{p}_r(x_i,y_j,z_k,t_l+d_t)+\hat{p}_r(x_i,y_j,z_k,t_l)]$$

3.3 Performance

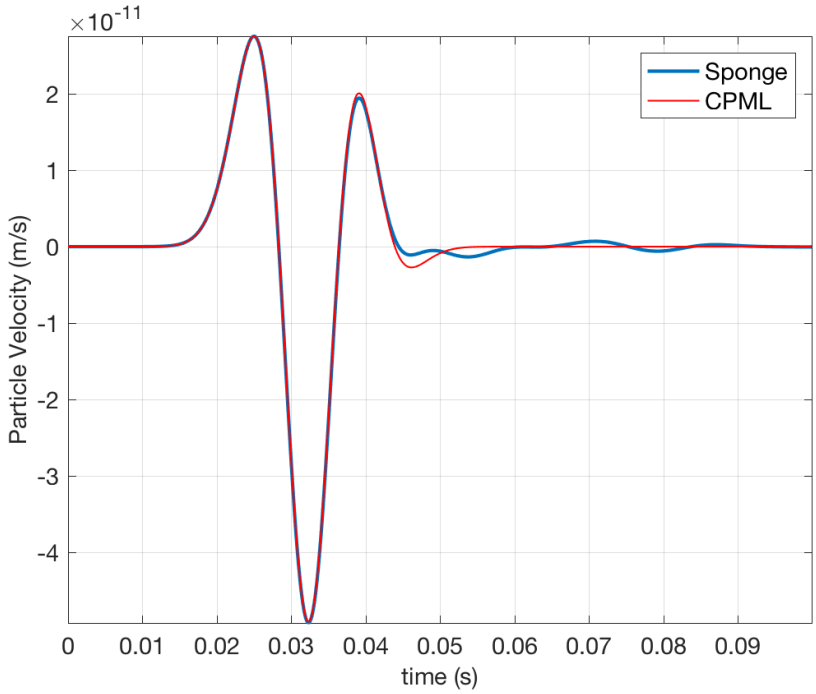

Figure 3: Comparison of Sponge and CPML absorbing boundary conditions for the X-component of particle velocity.

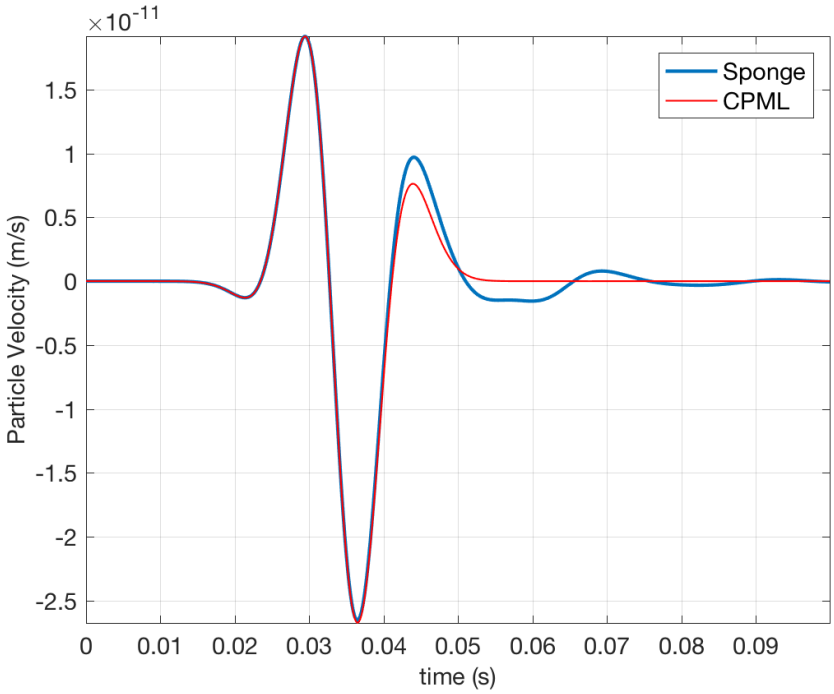

Figure 4: Comparison of Sponge and CPML for Z-component of particle velocity.

A vertical force source with a 100 Hz Ricker source-time-function was placed at the center of the grid and recorded 10 m below and offset 15 m in x for the sponge-MPML comparison. The comparison of the X, and Z particle velocities and pressure are shown in Figures 3-5. The Y-component is not shown due to the fact that along this recording plane, no Y particle velocity will be theoretically produced. As can be observed, the initial portion of the pulse is virtually identical between the two ABC conditions. However, discrepancies emerge in later portions of the pulse. Also, notice the continued fluctuations following the main pulse in the sponge case;

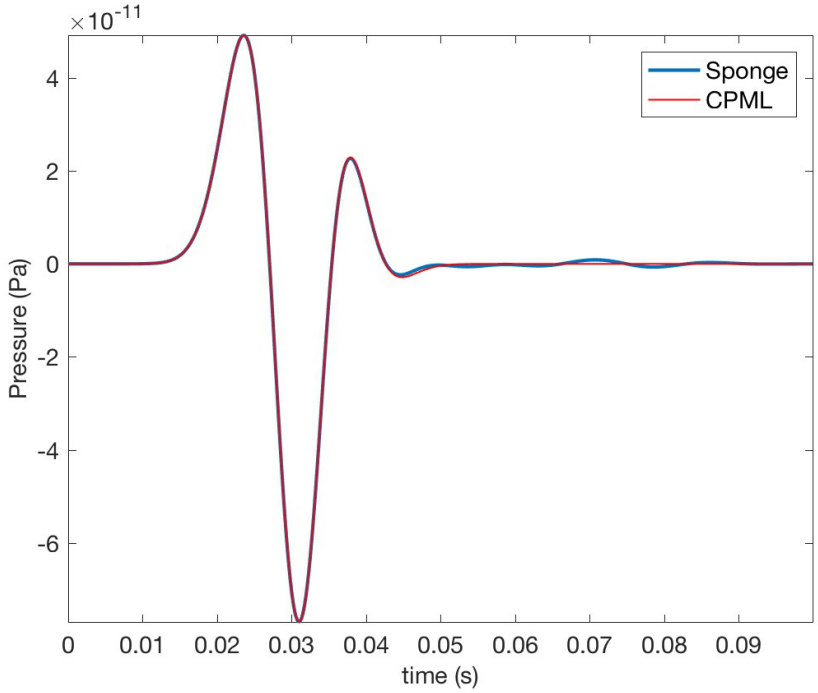

Figure 5: Comparison of Sponge and CPML for pressure.

these are reflections from the domain boundaries that we want to eliminate. The MPML has no noticeable deviations from zero following the main pulse, which is the correct, desirable result.

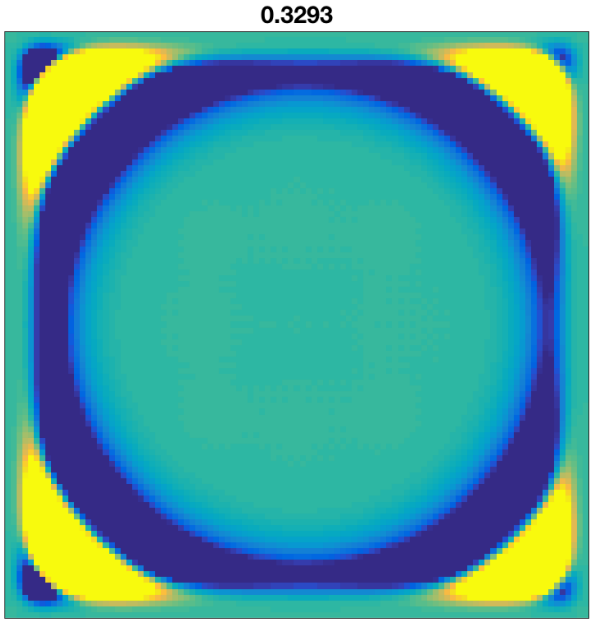

Figure 6: Demonstration of CPML performance in a homogeneous model on the XZ plane for pressure.

The absolute MPML performance example shows a snapshot of the pressure wavefield in the XZ plane at a time where the primary pulse is interacting with the MPML boundary zone (Figure 6). Note the very effective absorption of the wavefield at the boundary and little to no noticeable reflection back into the domain. The maximum outgoing amplitude impinging on the MPML zone is ~1e-4 Pa, whereas the maximum amplitude reflected back into the interior is ~1e-8 Pa, indicating a reflection coefficient on the order of 0.01%. This is greater than the theoretical reflection coefficient, but is still indicative of a superior absorbing boundary condition.

4. PHYSICS IMPROVEMENTS

4.1 Introduction

TDAAPS was originally designed for atmospheric acoustic modeling and, as such, includes some assumptions that are generally true in the atmosphere but may not be true in some other fluid media. Ostashev et al. (2005) derive the acoustic equations in full and also with several simplifying assumptions that are generally true in the atmosphere. The assumptions that TDAAPS makes is that 1) $\nabla \cdot \vec{v} = 0$, i.e., the fluid is incompressible, and 2) $\nabla P_0 = 0$, i.e., the spatial variation in the ambient medium pressure is small enough for acoustic wave propagation as to be negligible. The latter assumption definitely precludes computation of very long period atmospheric gravity waves, but TDAAPS also ignores temporal variations in density, which would be important for these types of waves as well. However, there may be instances, even in the atmosphere, especially where gradients in wind may be strong, that these terms may be important enough to retain. As such, a compile time flag (-DUSE_FULL_PRESSURE_UPDATING=1) is available that will use all the first-order (linear) terms in the moving media acoustic velocity-pressure system of equations. These additional terms only alter the pressure updating equations and, when used, add about 20% to the computation time. The default is to use the above two assumptions that apply most commonly in the atmosphere.

4.2 Theory

Ostashev et al. (2005) derive the moving acoustic equations in full and, thus, the derivation is not repeated here. The velocity updating equations remain as stated in Chapter 1; only the pressure updating equations are altered and are given by

$$\frac{\partial p}{\partial t} + \gamma p \frac{\partial v_k}{\partial x_k} + \kappa \frac{\partial w_k}{\partial x_k} + w_k \frac{\partial P_0}{\partial x_k} + v_k \frac{\partial p}{\partial x_k} = \frac{\partial e}{\partial t}$$

Where γ is the ratio of specific heats at constant pressure to constant volume. Note the symmetry in the ambient (v_k and P_0) and perturbation (w_k and p) terms. However, it would be desirable to eliminate P_0 from the above equations and this can accomplished using the assumption that the atmosphere (or other fluid medium) is in quasi-equilibrium among the ambient medium parameters. Thus, the gradient in ambient pressure P_0 can be rewritten in terms of gradients of the ambient wind. Using this assumption the above equation becomes

$$\frac{\partial p}{\partial t} + \gamma p \frac{\partial v_k}{\partial x_k} + \kappa \frac{\partial w_k}{\partial x_k} - \rho w_k v_j \frac{\partial v_k}{\partial x_j} + v_k \frac{\partial p}{\partial x_k} = \frac{\partial e}{\partial t}$$

This latter equation forms the basis for the numerical implementation in the following section.

4.3 Implementation

When all first-order terms in the moving acoustic equations are included, gradients of the ambient medium wind vectors are required for the pressure updating equations, similar to how they are used in the velocity updating equations. The following equations will redefine the D_{px} , D_{py} , and D_{pz} equations used in Section 3.2.6 to include all the linear terms. The remainder of the terms in Section 3.2.6 remain unchanged. Recall that within the interior of the domain, where no PML-type ABC is used, all the g_i terms are 0.

4.3.1 Pressure Updating Including All Linear Terms

$$D_{px}=-\hat{v}_x(x_i,y_j,z_k)\Big\{r_x[\hat{P}(x_i+d_x,y_j,z_k,t_l)-\hat{P}(x_i-d_x,y_j,z_k,t_l)]$$
$$+s_x[\hat{P}(x_i+2d_x,y_j,z_k,t_l)-\hat{P}(x_i-2d_x,y_j,z_k,t_l)]\Big\}$$
$$-\gamma\hat{P}(x_i,y_j,z_k,t_l)\Big\{c_x[\hat{v}_x(x_i+d_x,y_j,z_k)-\hat{v}_x(x_i-d_x,y_j,z_k)]\Big\}$$
$$+\rho(x_i,y_j,z_k)B_x(x_i,y_j,z_k,t_l)$$

where γ is the ratio of the specific heats at constant pressure to constant volume and is 1.4 for air. This medium parameter is currently constant throughout the computational domain, but could be upgraded to be position dependent in a future version. c_x are the 2nd order accurate coefficients for the gradient in the wind components

$$c_x=S_c\frac{d_t}{d_x}$$

The term B_x is

$$B_x(x_i,y_j,z_k,t_l)=\Big\{\bar{W}_x(x_i,y_j,z_k,t_l)\{c_x[\hat{v}_x(x_i+d_x,y_j,z_k)-\hat{v}_x(x_i-d_x,y_j,z_k)]\}$$
$$+\bar{W}_y(x_i,y_j,z_k,t_l)\{c_x[\hat{v}_y(x_i+d_x,y_j,z_k)-\hat{v}_y(x_i-d_x,y_j,z_k)]\}$$
$$+\bar{W}_z(x_i,y_j,z_k,t_l)\{c_x[\hat{v}_z(x_i+d_x,y_j,z_k)-\hat{v}_z(x_i-d_x,y_j,z_k)]\}\Big\}\hat{v}_x(x_i,y_j,z_k)$$

where

$$\bar{W}_x(x_i,y_j,z_k,t_l)=1/4\Big\{\hat{w}_x(x_i+d_x/2,y_j,z_k,t_l+d_t/2)+\hat{w}_x(x_i+d_x/2,y_j,z_k,t_l-d_t/2)$$
$$+\hat{w}_x(x_i-d_x/2,y_j,z_k,t_l+d_t/2)+\hat{w}_x(x_i-d_x/2,y_j,z_k,t_l-d_t/2)\Big\}$$
$$\bar{W}_y(x_i,y_j,z_k,t_l)=1/4\Big\{\hat{w}_y(x_i,y_j+d_y/2,z_k,t_l+d_t/2)+\hat{w}_y(x_i,y_j+d_y/2,z_k,t_l-d_t/2)$$
$$+\hat{w}_y(x_i,y_j-d_y/2,z_k,t_l+d_t/2)+\hat{w}_y(x_i,y_j-d_y/2,z_k,t_l-d_t/2)\Big\}$$
$$\bar{W}_z(x_i,y_j,z_k,t_l)=1/4\Big\{\hat{w}_z(x_i,y_j,z_k+d_z/2,t_l+d_t/2)+\hat{w}_z(x_i,y_j,z_k+d_z/2,t_l-d_t/2)$$
$$+\hat{w}_z(x_i,y_j,z_k-d_z/2,t_l+d_t/2)+\hat{w}_z(x_i,y_j,z_k-d_z/2,t_l-d_t/2)\Big\}$$

The remaining terms D_{py} and D_{pz} are

$$D_{py}=-\hat{v}_y(x_i,y_j,z_k)\Big\{r_y[\hat{P}(x_i,y_j+d_y,z_k,t_l)-\hat{P}(x_i,y_j-d_y,z_k,t_l)]$$
$$+s_y[\hat{P}(x_i,y_j+2d_y,z_k,t_l)-\hat{P}(x_i,y_j-2d_y,z_k,t_l)]\Big\}$$
$$-\gamma\hat{P}(x_i,y_j,z_k,t_l)\Big\{c_y[\hat{v}_y(x_i,y_j+d_y,z_k)-\hat{v}_y(x_i,y_j-d_y,z_k)]\Big\}$$
$$+\rho(x_i,y_j,z_k)B_y(x_i,y_j,z_k,t_l)$$
$$D_{pz}=-\hat{v}_z(x_i,y_j,z_k)\Big\{r_z[\hat{P}(x_i,y_j,z_k+d_z,t_l)-\hat{P}(x_i,y_j,z_k-d_z,t_l)]$$
$$+s_z[\hat{P}(x_i,y_j,z_k+2d_z,t_l)-\hat{P}(x_i,y_j,z_k-2d_z,t_l)]\Big\}$$
$$-\gamma\hat{P}(x_i,y_j,z_k,t_l)\Big\{c_z[\hat{v}_z(x_i,y_j,z_k+d_z)-\hat{v}_z(x_i,y_j,z_k-d_z)]\Big\}$$
$$+\rho(x_i,y_j,z_k)B_z(x_i,y_j,z_k,t_l)$$

with c_y and c_z similarly defined as c_x above and

$$B_y(x_i,y_j,z_k,t_l)=\Big\{\bar{W}_x(x_i,y_j,z_k,t_l)\{c_y[\hat{v}_x(x_i,y_j+d_y,z_k)-\hat{v}_x(x_i,y_j-d_y,z_k)]\}$$
$$+\bar{W}_y(x_i,y_j,z_k,t_l)\{c_y[\hat{v}_y(x_i,y_j+d_y,z_k)-\hat{v}_y(x_i,y_j-d_y,z_k)]\}$$
$$+\bar{W}_z(x_i,y_j,z_k,t_l)\{c_y[\hat{v}_z(x_i,y_j+d_y,z_k)-\hat{v}_z(x_i,y_j-d_y,z_k)]\}\Big\}\hat{v}_y(x_i,y_j,z_k)$$

$$B_z(x_i, y_j, z_k, t_l) = \Big[\bar{W}_x(x_i, y_j, z_k, t_l)\{c_z[\hat{v}_x(x_i, y_j, z_k + d_z) - \hat{v}_x(x_i, y_j, z_k - d_z)]\}$$
$$+\bar{W}_y(x_i, y_j, z_k, t_l)\{c_z[\hat{v}_y(x_i, y_j, z_k + d_z) - \hat{v}_y(x_i, y_j, z_k - d_z)]\}$$
$$+\bar{W}_z(x_i, y_j, z_k, t_l)\{c_z[\hat{v}_z(x_i, y_j, z_k + d_z) - \hat{v}_z(x_i, y_j, z_k - d_z)]\}\Big] \hat{v}_z(x_i, y_j, z_k)$$

with other terms as defined above.

4.4 Example

An example of the effect of the extra physics terms for a realistic atmospheric model is shown in Figure 7. This example is from a model with complex topography and 3-D variations in sound speed, density, and wind. On the large scale, there is little to no discernible difference between the traces when using or neglecting the extra physics terms. However, the inset shows a 10x enlargement of the trailing end of the primary pulse and its coda. Note the subtle differences are on the order of ~1% of the peak amplitude of the primary pulse.

4.5 Stability

The numerical stability of the original and augmented system of equations (with or without attenuation) is partially determined by the accuracy of the underlying ambient medium parameters. Implicit in the equations given throughout this document is that the ambient medium itself obeys the same physical and mathematical laws that are used to derive the acoustic equations. This, along with the assumption of quasi-equilibrium in the ambient medium, in turn implies a certain relationship exists among wind vectors and their gradients. If this is not true, then this disequilibrium may manifest itself as “sources” within the domain that will grow continually with time. Even very small disequilibria could eventually grow to large enough magnitude to make simulation results unusable given enough time. In practice, these disequilibria points arise most often within the atmosphere right above the topography. These are indeed the areas that would be suspected to have the highest likelihood of error either directly due to codes that compute ambient media states or introduced during interpolation of those models onto the TDAAPS grid. Wind gradients are also large near the topographic surface, which also increases the likelihood for error. The terms added in this chapter are relatively small except in areas with large wind gradients, such as near the surface. Indeed, when all linear terms are included, there tends to be fewer and slower growing disequilibria points than when they are not used. However, even using the full updating equation for pressure does not eliminate this problem completely.

Another tactic that is used to mitigate against disequilibria points is to ensure that nodes right next to topography do not smear wind gradients into regions, such as the solid earth, where the wind and wind gradients should be zero. The finite-difference equations average (either arithmetically or harmonically) medium parameters for equations that do not directly reside at the storage location for the parameters they are differencing or averaging. TDAAPS will force wind gradients to be zero for updating points whose harmonically averaged density is greater than $500/S_\rho$. Obviously, this was designed for the atmosphere but could be altered to apply to any fluid where there is a reasonably great density contrast, but as the density contrast reduces it is expected that the amount of disequilibrium would decrease and so become less of an issue.

It should be noted that TDAAPS employs the "order-switching" formalism introduced in Preston et al. (2008) that reduces the finite-difference order from 4th to 2nd order in space for nodes adjacent to high contrast interfaces such as occurs at the air-earth interface. This is required for stability and for accuracy.

Finally, when attenuation is used in the model, it will mitigate against these disequilibria instabilities since it naturally attenuates these numerically growing "sources." How much attenuation may be necessary to eliminate these instabilities will depend on the wind gradient near the topography and it may in some circumstances be completely eliminated by the actual attenuation in the medium. In other instances, however, unrealistically large attenuation may be required to eliminate these instabilities and other methods may need to be explored to fully eliminate this problem.

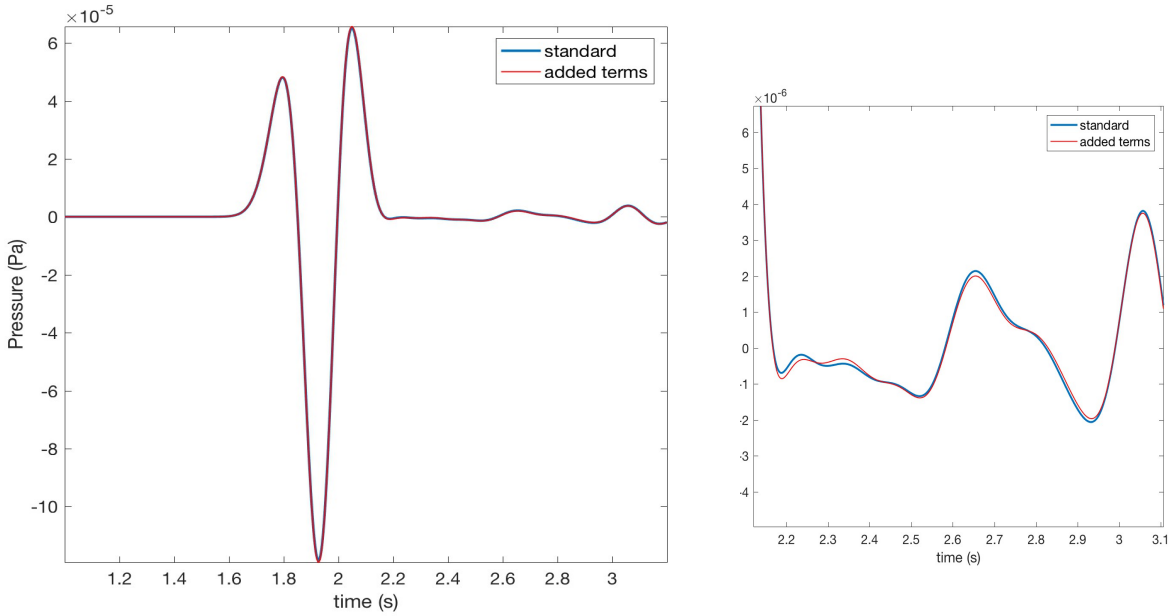

Figure 7: Effects of using all the first order terms in a realistic atmospheric model. "Standard" refers to the usual method of neglecting terms, whereas "added terms" refers to the inclusion of all first order terms. The right inset shows a 10x enlargement of the tail end of the primary pulse and coda.

5. DETERMINING ATTENUATION PARAMETERS

5.1 Introduction

As mentioned in Chapter 2, there are 2*R parameters that must be given in order to define an attenuation model: R a_r amplitude scalars and R ω_r decay frequencies. This chapter shows how one determines these parameters given a loss versus frequency curve. This will be demonstrated for a typical atmospheric acoustic loss function and for seawater.

5.2 Theory

The definition of an attenuation mechanism is provided in Section 2.2. However, how do these attenuation mechanisms defined in terms of acoustic moduli relate to loss versus frequency? Aldridge (in prep) also derives the loss versus frequency given a standard linear solid that we can utilize to obtain acoustic loss versus frequency. First define two functions in the frequency domain

$$A(f)=\sum_{r=1}^{R}\frac{a_r}{1+(\omega/\omega_r)^2}$$

$$B(f)=\sum_{r=1}^{R}\frac{a_r(\omega/\omega_r)}{1+(\omega/\omega_r)^2}$$

Then the attenuation function is defined as

$$\alpha(f)=\frac{\omega}{c_\infty}\sqrt{\frac{\sqrt{(1-A(f))^2+B(f)^2}-(1-A(f))}{2[(1-A(f))^2+B(f)^2]}}$$

where c_∞ is the phase speed at infinite frequency ($c_\infty=\sqrt{\kappa/\rho}$). The units are 1/length, which typically, with the sound speed given as m/s, will be 1/m. This also implies that the phase speed is a function of frequency and is given by

$$c(f)=c_\infty\sqrt{\frac{2[(1-A(f))^2+B(f)^2]}{\sqrt{(1-A(f))^2+B(f)^2}+(1-A(f))}}$$

Given an $\alpha_{true}(f)$ one can find the R a_r and R ω_r that will produce an attenuation function $\alpha(f)$ above that best fits the true one in some sense. The Matlab function acousticAttenSeek.m takes a vector of frequencies where $\alpha_{true}(f)$ is known, the $\alpha_{true}(f)$ at those frequencies, the phase speed at infinite frequency, the number of attenuation mechanisms that you want (R), and a reference frequency. It will output R amplitude scalars and R decay frequencies as well as the ratio of the phase velocity at the reference frequency to that at infinite frequency that best fit the input loss function in a least squares sense.

Of course, this solution is purely mathematical, and does not know anything about any physical limitations on these output parameters. All of the amplitude scalars and decay rates must be real, positive numbers as the most general restriction. Beyond that, there are rules that should be true in order for them to represent a physical system bounds by the constraints of causality. One obvious constraint is that $c(0)$ must be real and positive. This places the constraint that

$$\sum_{r=1}^{R}a_r<1$$

Other than this simple constraint, the general requirements for arbitrary R mechanisms is not known. In practice, the author is not aware of any output from acousticAttenSeek.m for any attenuation model that fits the basic constraints above that appear to violate causality, but, of

course, this does not mean that a model doesn't exist that would produce parameters that are physically impossible. The most likely result of a physically impossible attenuation model would be instability of the solution.

5.3 Atmospheric Attenuation Example

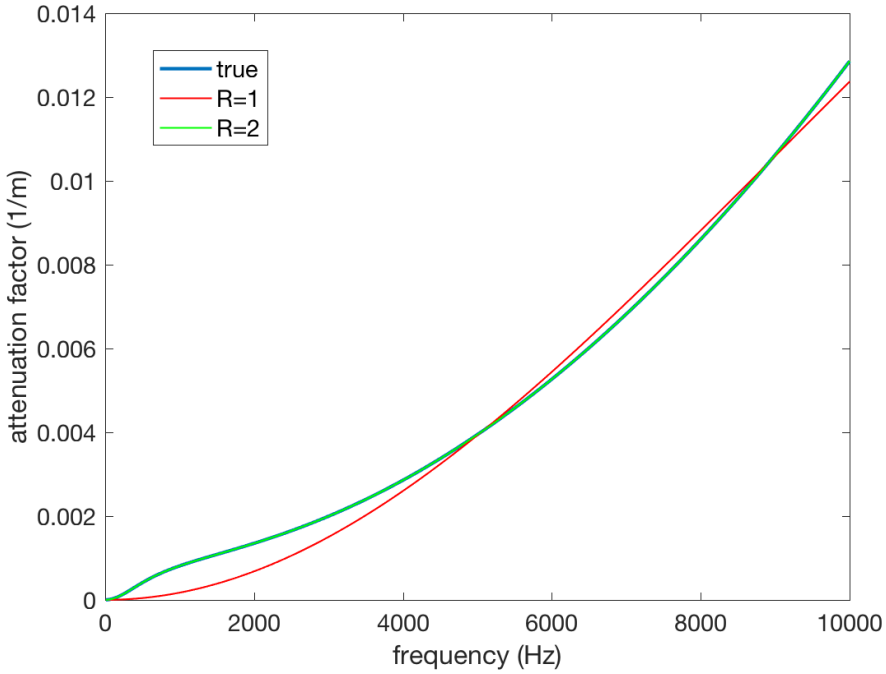

Figure 8: Acoustic attenuation factor fits for a 1 and 2 mechanism model.

The Matlab code acousticAtten.m computes the attenuation (1/m) as a function of frequency based on the ISO 9613-1 (1993) standard. Figure 8 shows the ISO standard attenuation over the frequency range 10 Hz to 10 kHz compared to the best fit in a least squares sense attenuation model with 1 and 2 mechanisms. The fit is excellent for a 2 mechanism model, meaning that this model would be an adequate representation of the physical attenuation over this frequency range. The 1-mechanism model is unable to fit some of the curve's variations in this band.

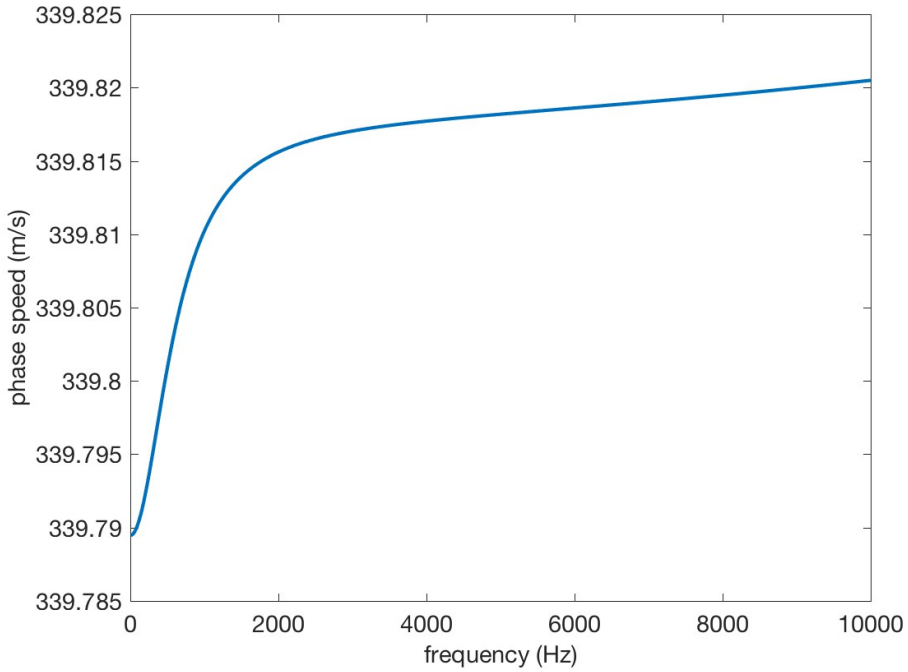

Figure 9: Sound speed dispersion implied by the 2 mechanism model.

Figure 9 shows the subtle phase speed dependence on frequency for the 2-mechanism model.

5.4 Seawater Attenuation Example

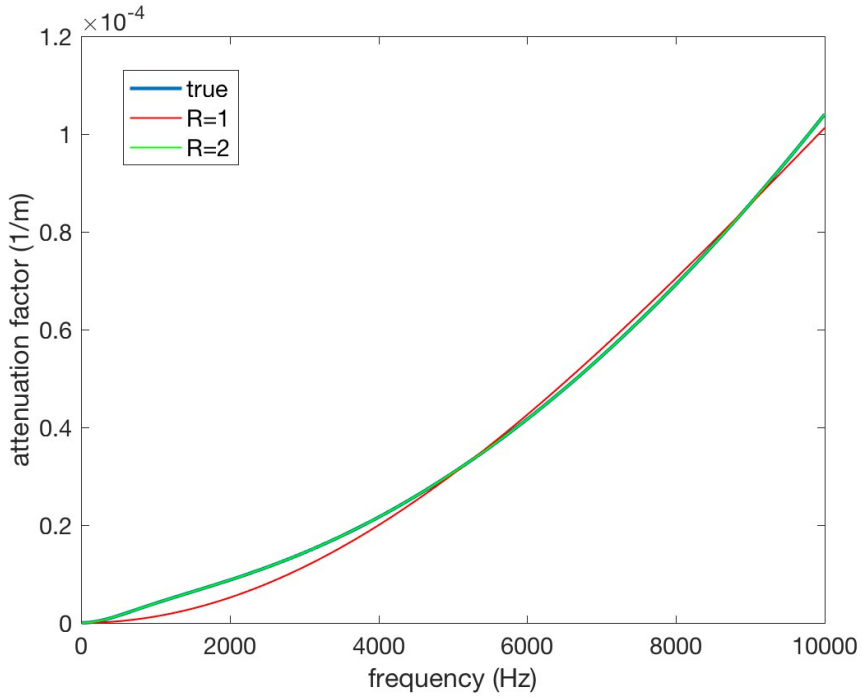

Figure 10: Seawater attenuation factor fits for 1- and 2-mechanism attenuation models.

The Matlab code seawaterAtten.m also computes the attenuation (1/m) as a function of frequency for seawater. This is based on equations given in Ainslie and McColm (1998) that use only the physical loses due to pure water, boric acid, and magnesium sulfate, which are the primary contributors to attenuation in seawater in the Hz to kHz range. Figure 10 shows the Ainslie and McColm attenuation model over the frequency range 10 Hz to 10 kHz and the best fit 1 and 2 mechanism attenuation models. Once again, the fit is excellent over this bandwidth for the 2 mechanism model, whereas the 1 mechanism model cannot fit the inflections of the curve.

6. VALIDATION TESTS

6.1 Introduction

Code validation is important to help verify that the physics and the code implementation of the physics give expected results. One means of validation is comparison of results of two different codes under the same conditions. Validation of TDAAPS 2 was made against two different codes. The original TDAAPS, which is a non-attenuative code, was used to validate TDAAPS 2 in the case that the attenuation parameters are used but set to coincide with a non-attenuative model. To test the attenuation aspect of the code, the new code was tested against Parelasti, the Geophysics Department's finite-difference anelastic algorithm in the case of fixed medium for TDAAPS and zero shear wave speed for Parelasti with identical attenuation parameters. A moving acoustic, attenuative comparison was not made since no codes were available for testing.

For these test cases a simple homogeneous acoustic model was used. The sound speed and density were set to 2500 m/s and 2000 kg/m^3, respectively, for comparisons with Parelasti. The non-attenuative models used a homogeneous sounds speed of 340 m/s and density of 1.2 kg/m^3.

6.2 Non-Attenuative Acoustic Comparison

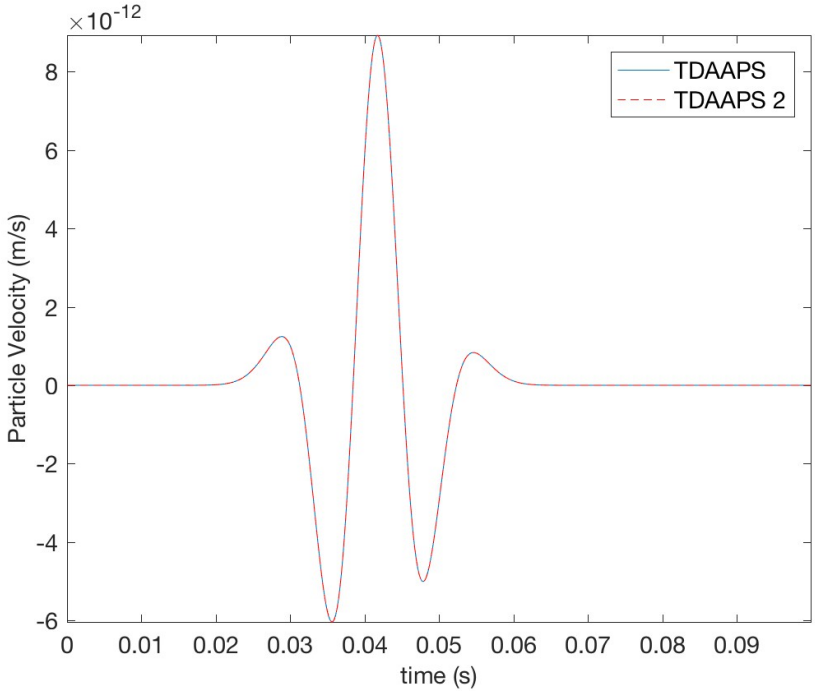

Figure 11: X-component of velocity comparison for fixed acoustic models.

The purpose of these comparisons is to test whether the attenuation code reduces to the non-attenuative output when attenuation parameters are set to zero. Two basic test cases were considered. The first consisted of a fixed media (no wind) model comparison between the original TDAAPS without attenuation and TDAAPS 2 with attenuation turned on, but all amplitude factors set zero, meaning that the attenuation portion of the code is exercised, but no attenuation will result. Figures 11-13 shows the excellent comparison of the two codes in the case of a vertical point source in the center of the grid using a 10 Hz Ricker wavelet source-time-

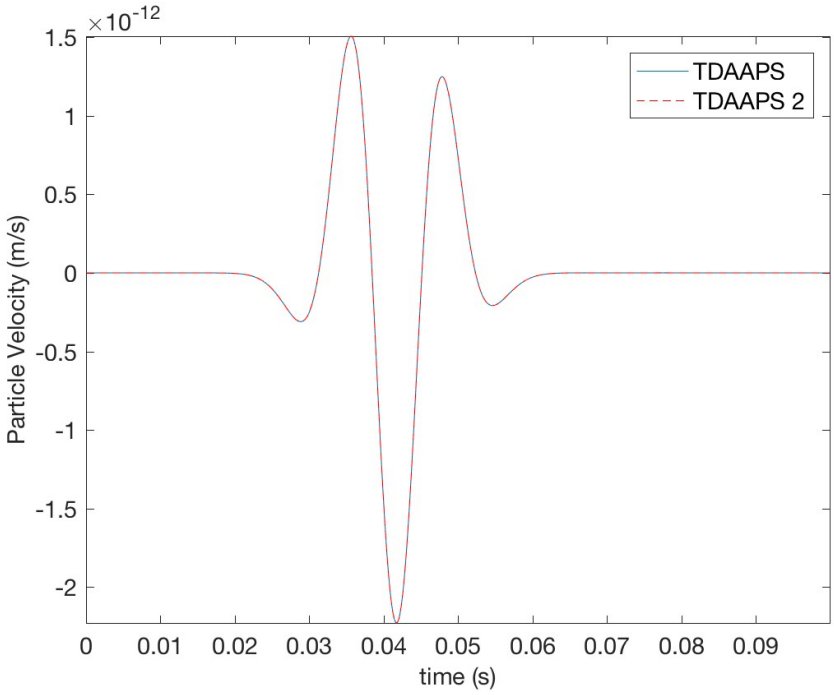

Figure 12: Z-component of velocity comparison for fixed acoustic model.

function recorded 10 m below and 40 m offset in the X direction for the X-component of velocity, Z-component of velocity, and pressure. The Y-component of velocity is theoretically zero.

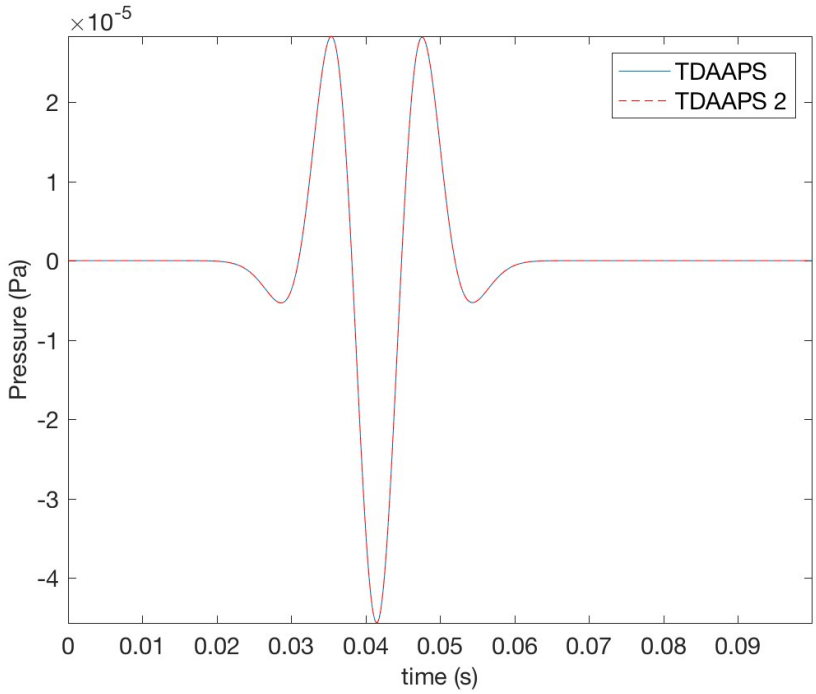

Figure 13: Pressure comparison for fixed acoustic model.

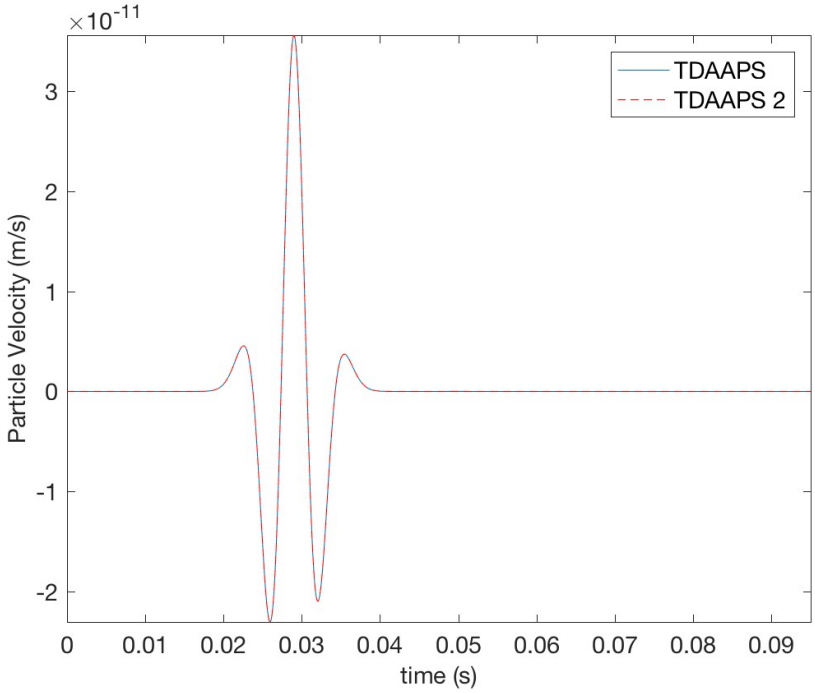

Figure 14: X-component velocity comparison with wind model.

The second case is a moving media case with the same homogeneous sound speed and density model. The wind is a vortex centered at the center of the grid with wind speed increasing radially to a Mach number (wind speed/sound speed) of 0.20, a very strong wind. The same source and receiver locations were used as in the first case. Comparisons are also excellent on all components of velocity and pressure (Figures 14-17). Note that the Y-component of particle velocity is also shown, since, due to the wind, there will be detectable signal on this component.

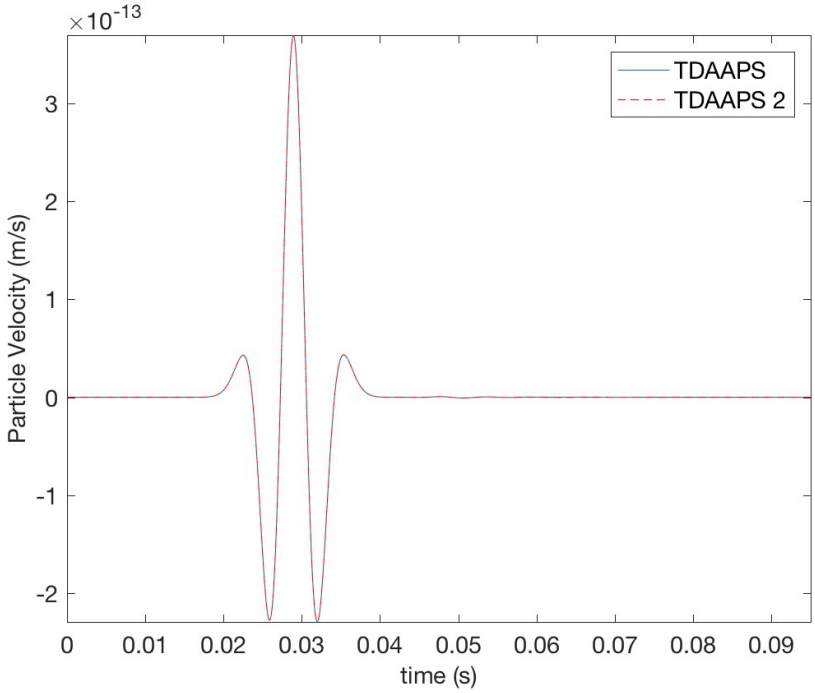

Figure 15: Y-component of velocity comparison for wind model.

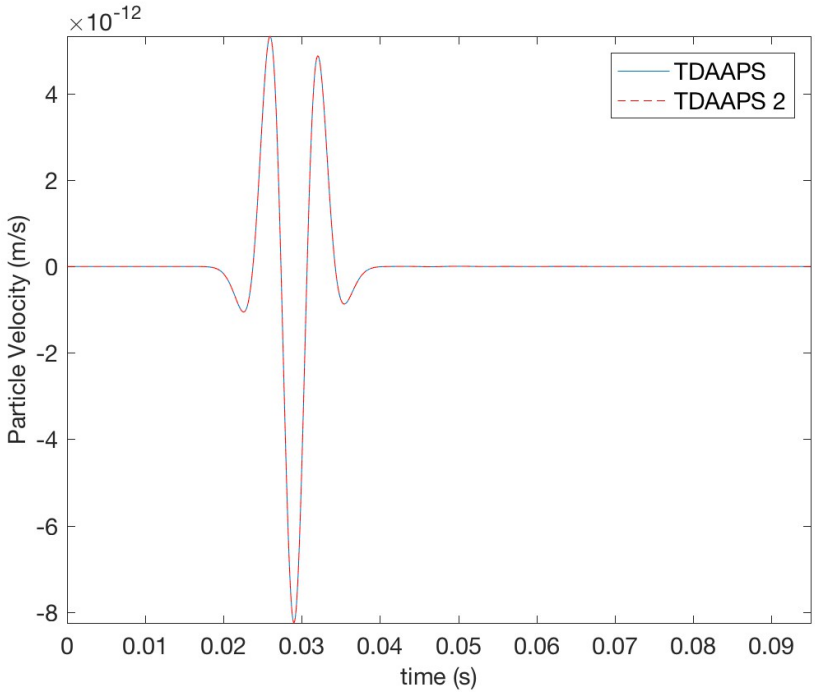

Figure 16: Z-component of velocity comparison for wind model.

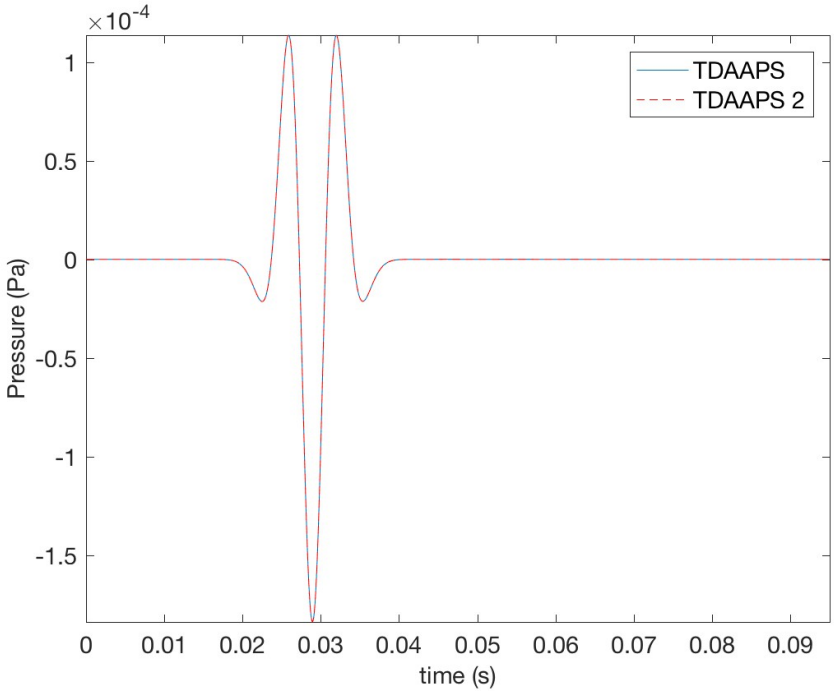

Figure 17: Pressure comparison for wind model.

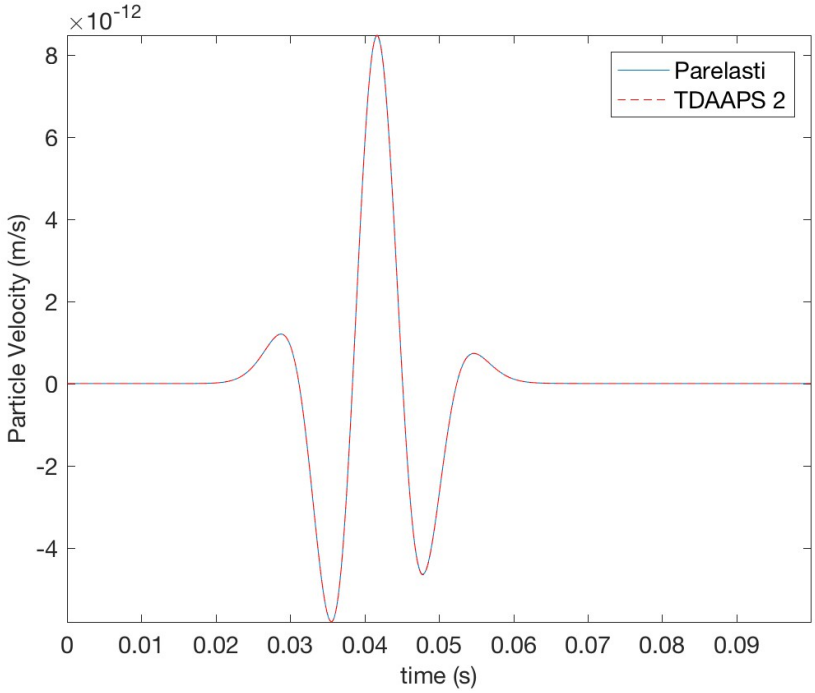

Figure 18: X-component of velocity comparison for attenuative model.

6.3 Fixed Acoustic Attenuative Medium Comparison

This comparison tests the attenuation acoustic code to ensure that it gives the same answers as Parelasti using an anelastic model with the shear wave speed set to zero. We used attenuation parameters appropriate for a seismic model with an equivalent Q of 100 for 2 attenuation mechanisms. The relaxation frequencies and amplitude factors utilized were 3.061493 Hz with amplitude 0.025949 for the first and 66.091248 Hz with amplitude 0.018347 for the second. A 100 Hz Ricker source-time-function vertical force source located at the center of the grid was recorded 10 m below and 40 m offset in X for the X-component of particle velocity, Z-component of velocity, and pressure. Again, note that the Y-component of velocity is theoretically zero for this configuration of source and receiver. Agreement between the two codes is excellent on all traces (Figures 18-20).

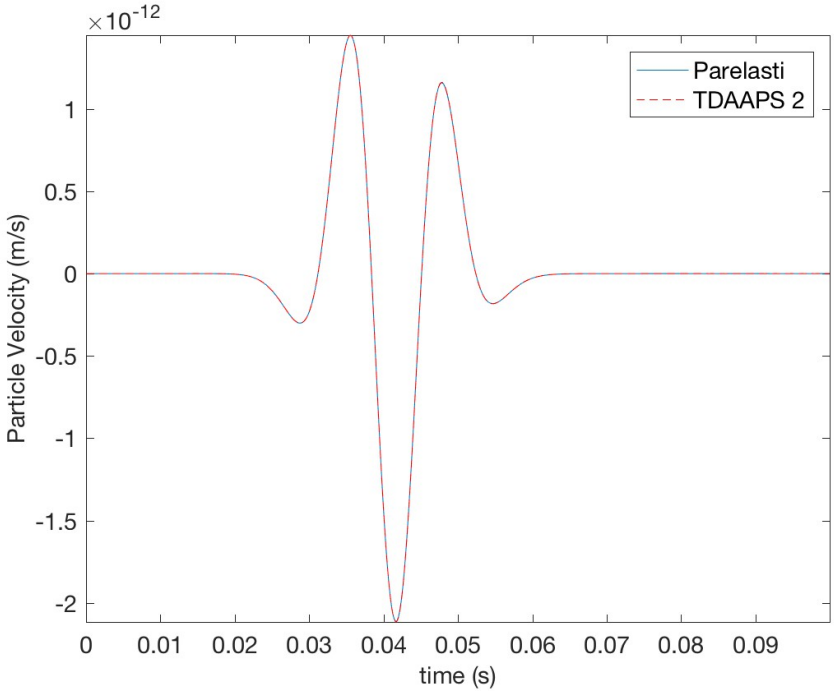

Figure 19: Z-component of velocity comparison for attenuative model.

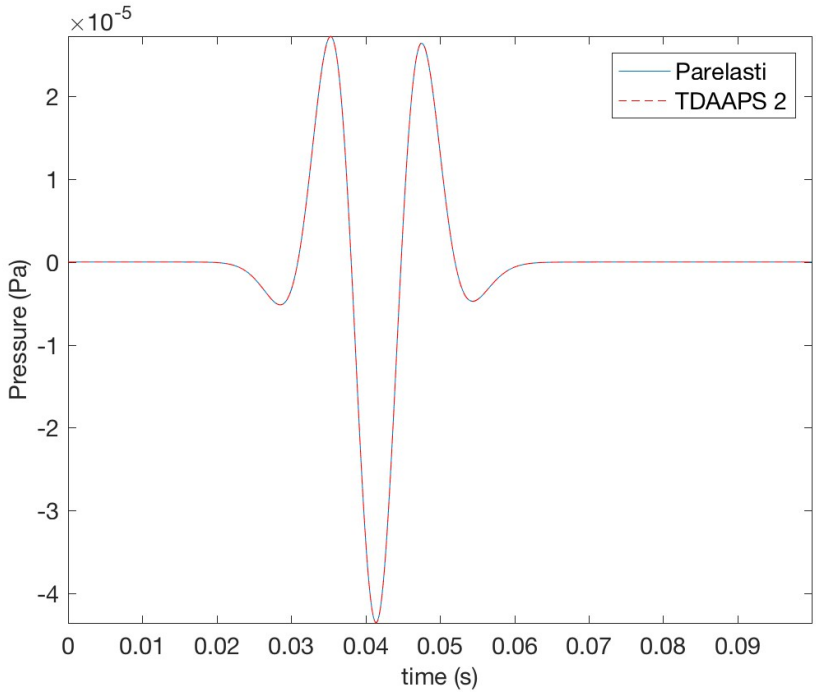

Figure 20: Pressure comparison for attenuative model.

7. CONCLUSIONS

We have outlined improvements that have been made to TDAAPS in order to model acoustic wave propagation in attenuative, moving media which can include realistic 3-D atmospheric conditions and topography. In addition, improved absorbing boundary conditions allow more accurate simulation results in a smaller computational domain, saving resources and time. The optional usage of all the linear terms in the linear acoustic wave equations does mitigate against instabilities in the solution in some cases and expands the capability of acoustic modeling beyond air or water to other materials in which these terms could not be neglected. Methods for computing the attenuation parameters from desired attenuation factor versus frequency response were also provided. Finally, the improved code, TDAAPS 2, has been validated against the original TDAAPS in non-attenuative cases and against an anelastic solver.

8. REFERENCES

1. Ainslie, M.A., and G.J. McColm, A simplified formula for viscous and chemical absorption in seawater, *J. Acousti. Soc. Am.*, 103 (3), 1671-1672, 1998.
2. Aki, K., and P.G. Richards, *Quantitative Seismology*, 2nd Edition, Univ. Sci. Books, Sausalito, CA, 2002.
3. Aldridge, D.F., and M.M. Haney, *Numerical Dispersion for the Conventional-Staggered-Grid Finite-Difference Elastic Wave Propagation Algorithm*, SAND2008-4991, Sandia National Laboratories, Albuquerque, NM, July 2008.
4. Berenger, J-P., A Perfectly Matched Layer for the Absorption of Electromagnetic Waves, *J. Comp. Phys.*, 114, 185-200, 1994.
5. Cerjan, C., D. Kosloff, R. Kosloff, and M. Reshef, A Non-Reflecting Boundary Condition for Discrete Elastic and Acoustic Wave Equations, *Geophys.*, 50 (4), 705-708, 1985.
6. ISO 9613-1: *Acoustics -- Attenuation of sound during propagation outdoors -- Part 1: Calculation of the absorption of sound by the atmosphere*, ISO, Geneva, Switzerland, 1993.
7. Komatitsch, D., and R. Martin, An Unsplit Convolutional Perfectly Matched Layer Improved at Grazing Incidence for the Seismic Wave Equation, *Geophys.*, 72 (5), SM155-SM167, doi 10.1190/1.2757586, 2007.
8. Meza-Fajardo, K.C., and A.S. Papageorgiou, A Nonconvolutional, Split-Field, Perfectly Matched Layer for Wave Propagation in Isotropic and Anisotropic Elastic Media: Stability Analysis, *Bull. Seis. Soc. Am.*, 98 (4), 1811-1836, doi: 10.1785/0120070223, 2008.
9. Ostashev, V.E., D.K. Wilson, L. Liu, D.F. Aldridge, N.P. Symons, and D. Martin, Equations for Finite-Difference, Time-Domain Simulations of Sound Propagation in Moving Inhomogeneous Media and Numerical Implementation, *J. Acousti. Soc. Am.*, 117 (2), 503-517, 2005.
10. Preston, L.A., D.F. Aldridge, N.P. Symons, Finite-Difference Modeling of 3D Seismic Wave Propagation in High-Contrast Media, *Soc. Expl. Geophys. 2008 Annual Meeting Extended Abstracts*, 2008.
11. Symons, N.P., D.F. Aldridge, D.H. Marlin, S.L. Collier, D.K. Wilson, V.E. Ostashev, *Modeling with the Time-Domain Atmospheric Acoustic Propagation Suite (TDAAPS)*, SAND2006-2540, Sandia National Laboratories, Albuquerque, NM, May 2006.

DISTRIBUTION

1	MS0750	Leiph Preston	6911
1	MS0899	Technical Library	9536 (electronic copy)


Sandia National Laboratories